Disruption research on Alcator C-Mod

Three topics:

1) High resolution halo current measurements using Langmuir probes
2) Runaway electron synchrotron emission
   - Spectra and energy at 2.7, 5.4, & 7.8 tesla
   - Synthesizing images of RE beams
3) Databases for disruption warning analysis, including applications of machine learning

ITER school on disruptions and control
Aix-en-Provence
2017/03/20-25

Alcator C-Mod

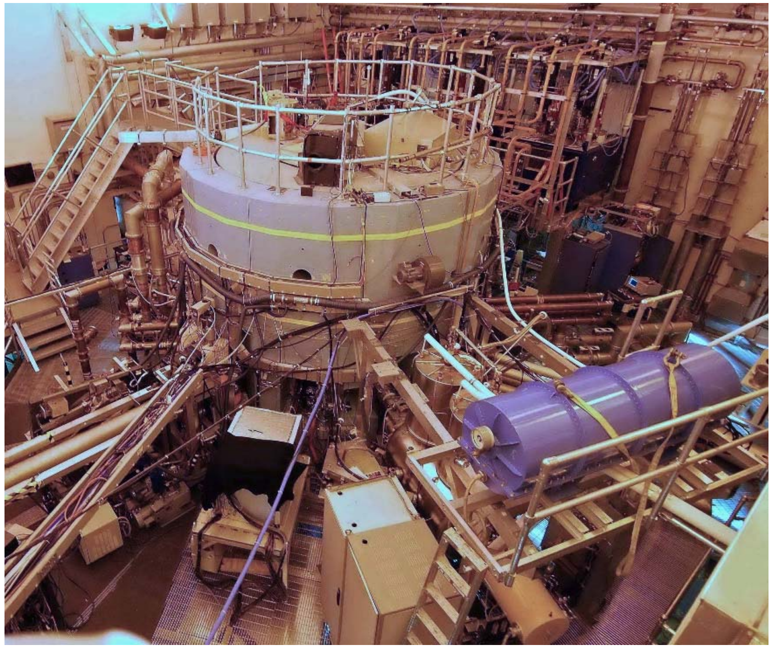

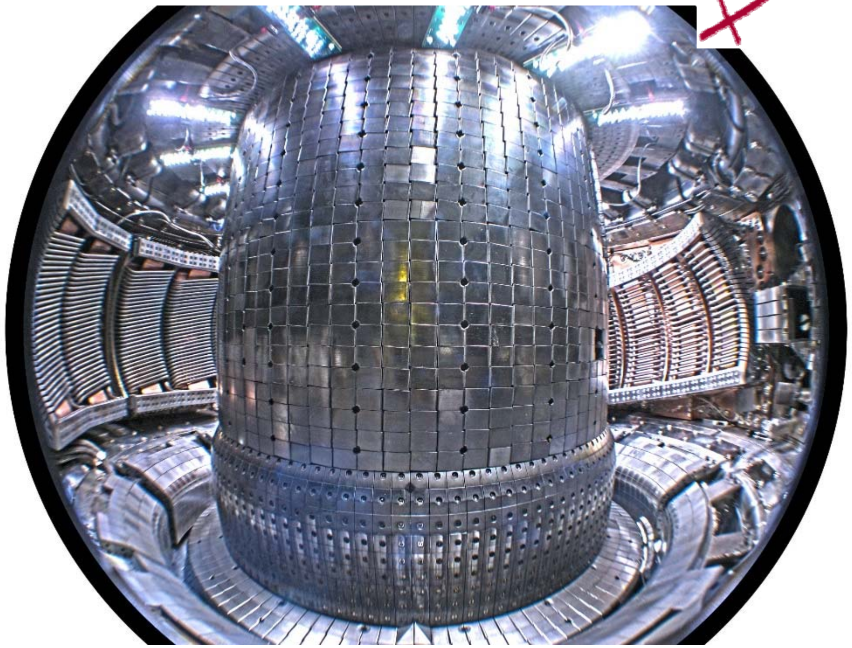

- High field ($B \leq 8$ T), high current ($I_p \leq 2$ MA), high energy density ($W_{th}/Vol \leq 0.3$ MJ/m^3, $\langle p \rangle \leq 2$ atm), compact size ($R_0 = 0.68$ m)
- ***These characteristics greatly exacerbate disruption effects***
  - Equipped with extensive disruption-relevant diagnostics
  - Equipped with two massive gas injection (MGI) systems for disruption mitigation studies
- C-Mod permanently shut down last year

Images from a typical C-Mod disruption

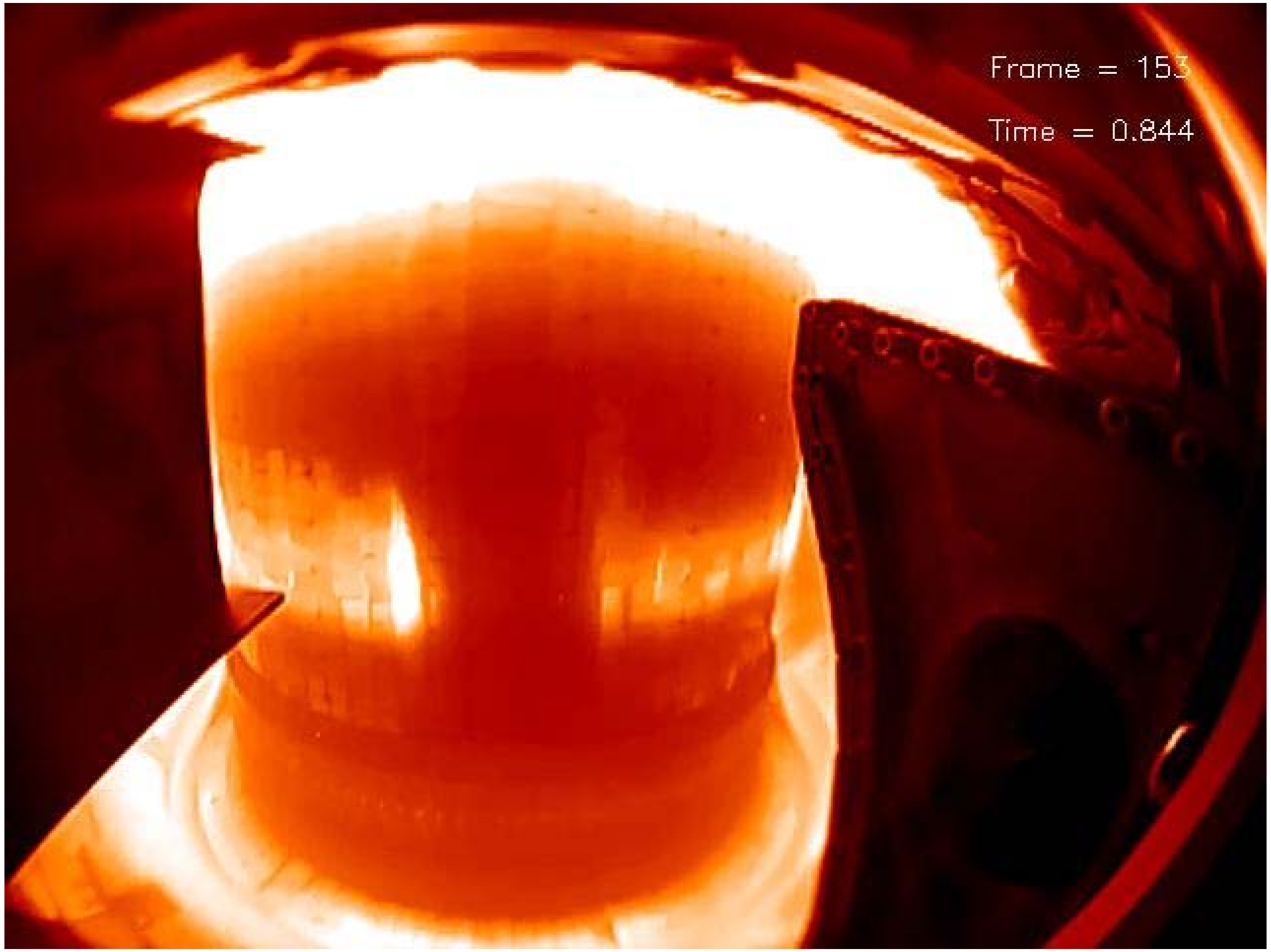

Video from a typical C-Mod disruption

Images from a typical C-Mod disruption

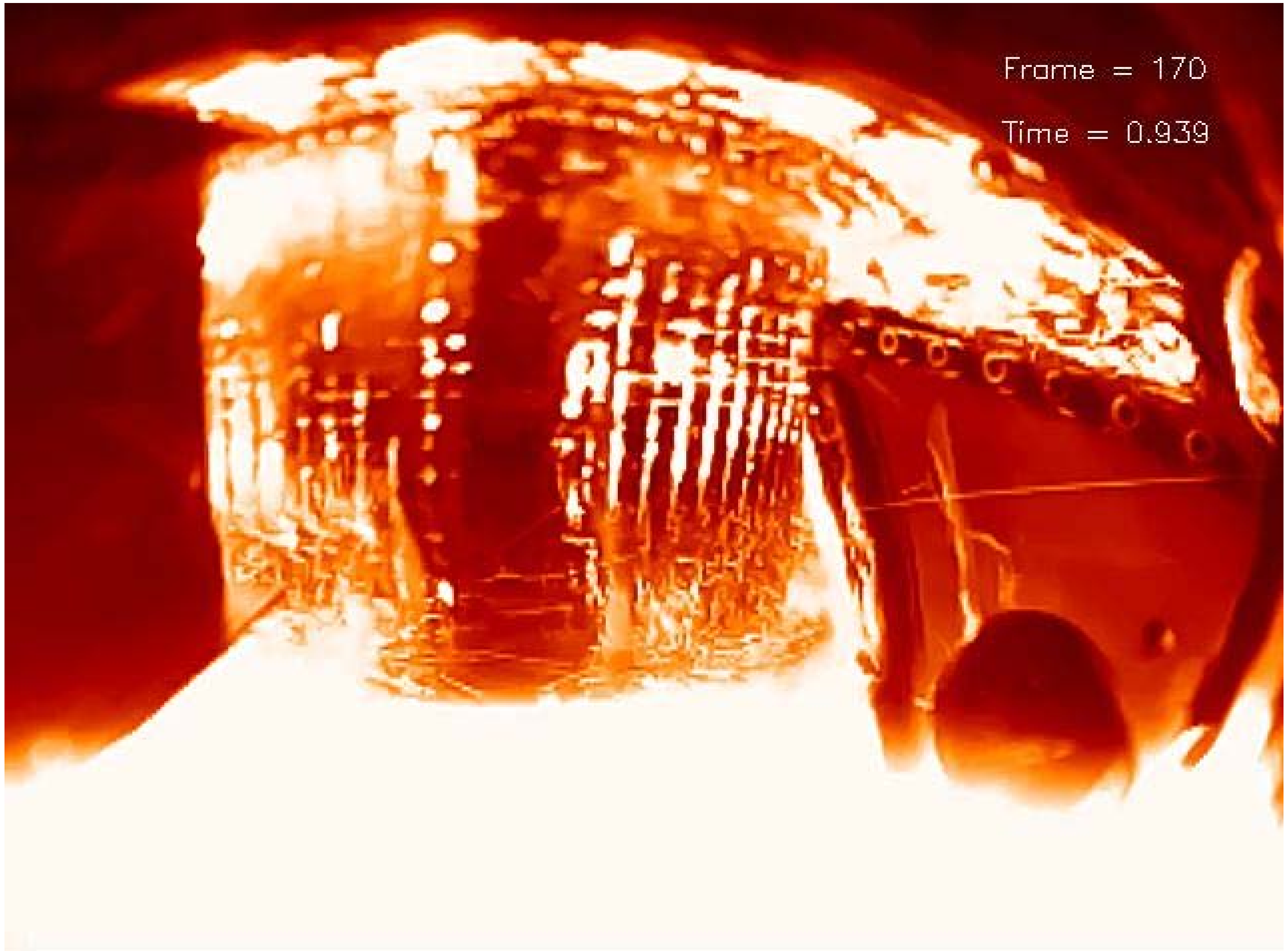

Images from a typical C-Mod disruption

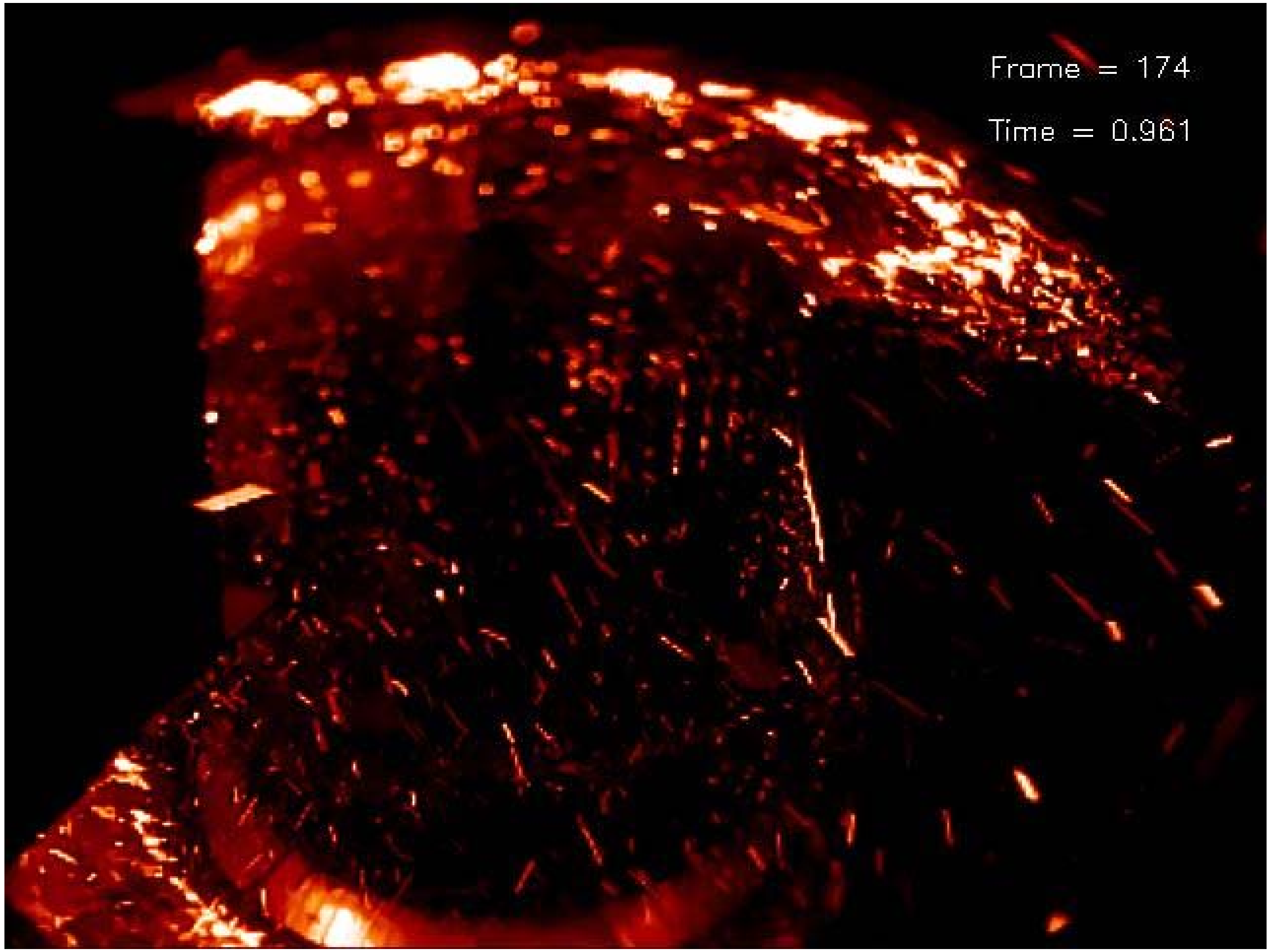

Disruption research on Alcator C-Mod

Three topics:

1) High resolution halo current measurements using Langmuir probes
2) Runaway electron synchrotron emission
   - Spectra and energy at 2.7, 5.4, & 7.8 tesla
   - Synthesizing images of RE beams
3) Databases for disruption warning analysis, including applications of machine learning

High Resolution Halo Current Measurements using Langmuir Probes in Alcator C-Mod

R. Granetz, A. Tinguely, A. Berg,
A. Kuang, D. Brunner, B. LaBombard

MIT Plasma Science and Fusion Center

Disruption halo currents have been measured on tokamaks for many years

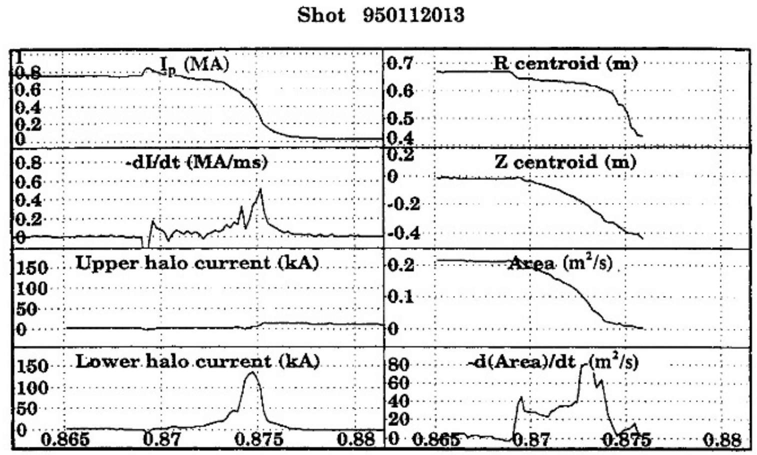

FIG. 2. Evolution of the plasma current, halo currents, position and cross-sectional area during the thermal quench disruption shown in Fig. 1(a).

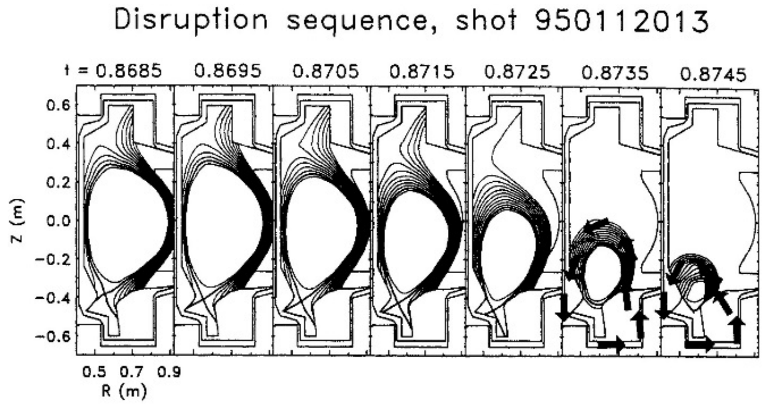

FIG. 3. Magnetic flux reconstructions at 1 ms intervals for the disruption shown in Fig. 1(a). The arrows show the poloidal projection of halo current flow, which exists primarily during the last two frames. In order to be force-free, the portion of the halo circuit in the plasma scrape-off must actually follow a helical path.

R. Granetz, *et al*, Nucl. Fusion **36**, 1996

Halo currents have traditionally been measured with Rogowski sensors and/or current shunts

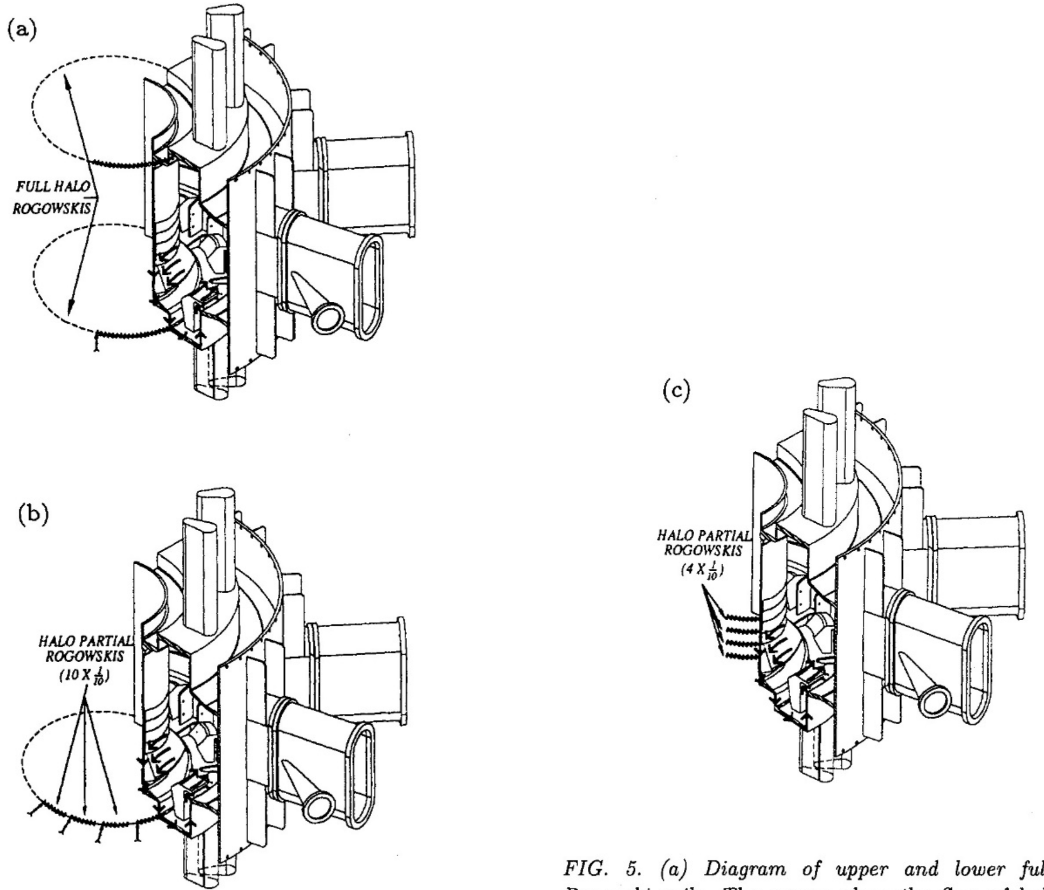

FIG. 5. (a) Diagram of upper and lower full halo Rogowski coils. The arrows show the flow of halo current into and out of the vessel surface, and through the Rogowski coils. (b) Diagram of toroidal array of ten halo Rogowski segments. (c) Diagram of vertical array of four halo Rogowski segments.

R. Granetz, *et al*, Nucl. Fusion **36**, 1996

Halo currents have traditionally been measured with Rogowski sensors and/or current shunts

Mechanical constraints limited measurement resolution in the poloidal dimension to ~10 cm

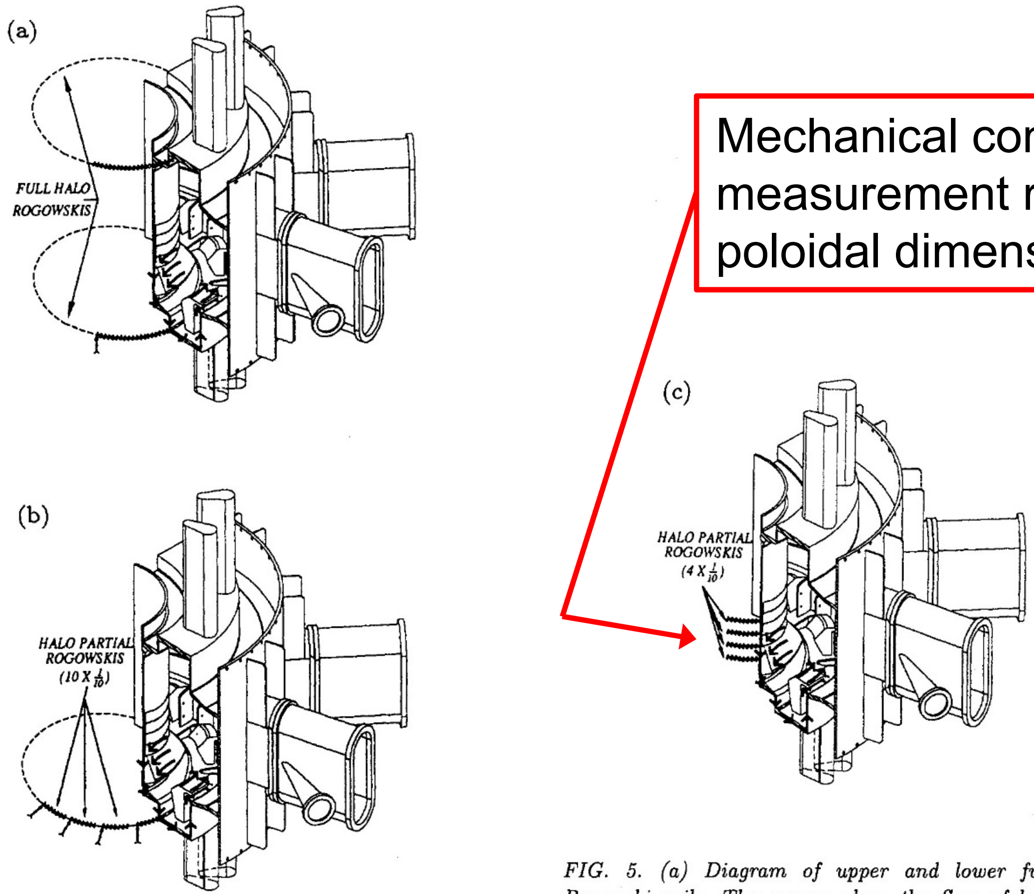

FIG. 5. (a) Diagram of upper and lower full halo Rogowski coils. The arrows show the flow of halo current into and out of the vessel surface, and through the Rogowski coils. (b) Diagram of toroidal array of ten halo Rogowski segments. (c) Diagram of vertical array of four halo Rogowski segments.

R. Granetz, *et al*, Nucl. Fusion **36**, 1996

New SOL diagnostic: Langmuir rail probes

- 21 flush-mounted Langmuir rail probes give SOL profiles from bottom to top of outboard divertor plate with fast time resolution

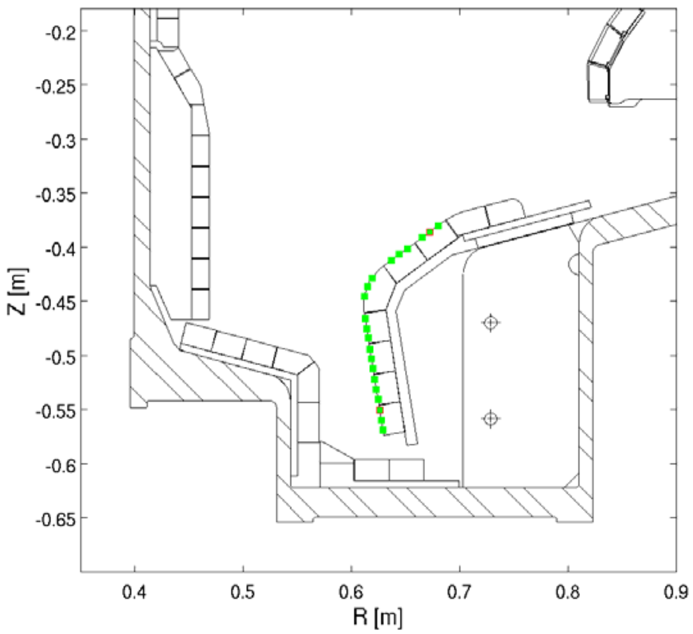

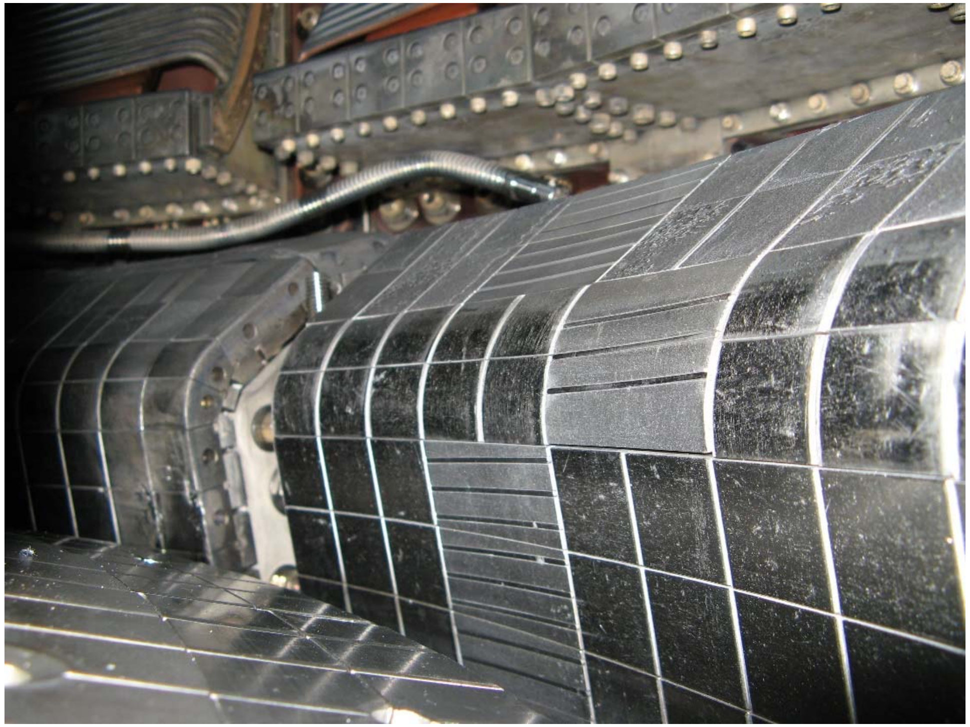

New SOL diagnostic: Langmuir rail probes

- 21 flush-mounted Langmuir rail probes give SOL profiles from bottom to top of outboard divertor plate with fast time resolution
- Primarily intended to measure I-V characteristics to provide $T_e(\psi)$, $n_e(\psi)$, and $V_f(\psi)$ in the SOL at the outboard divertor plate

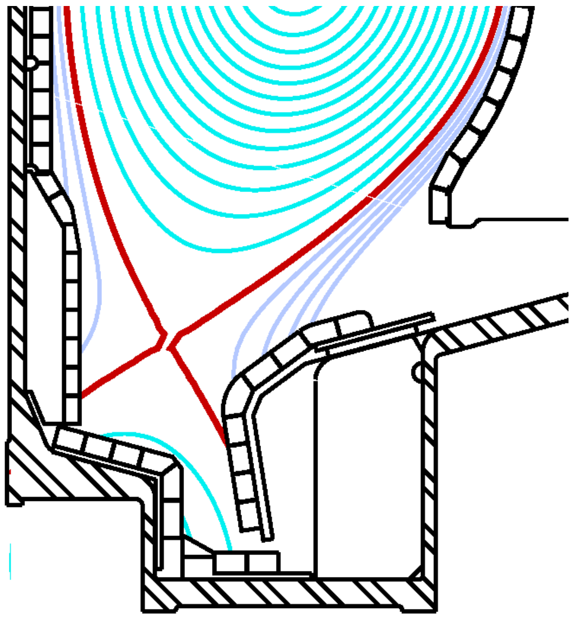

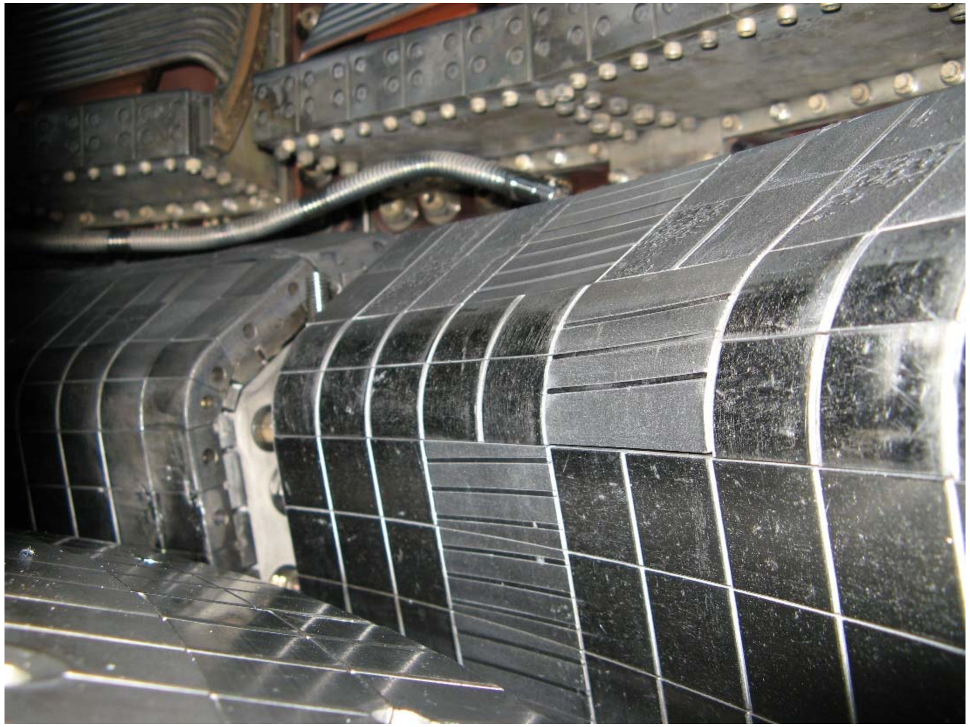

New SOL diagnostic: Langmuir rail probes

- When run in "grounded" mode, the probes appear to the plasma to just be part of the divertor plate surface (almost)
- Current flowing in/out of the probes can be measured while in grounded mode.

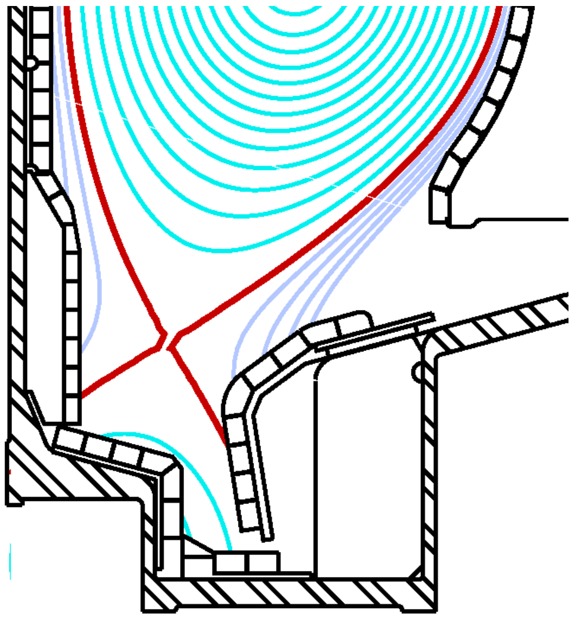

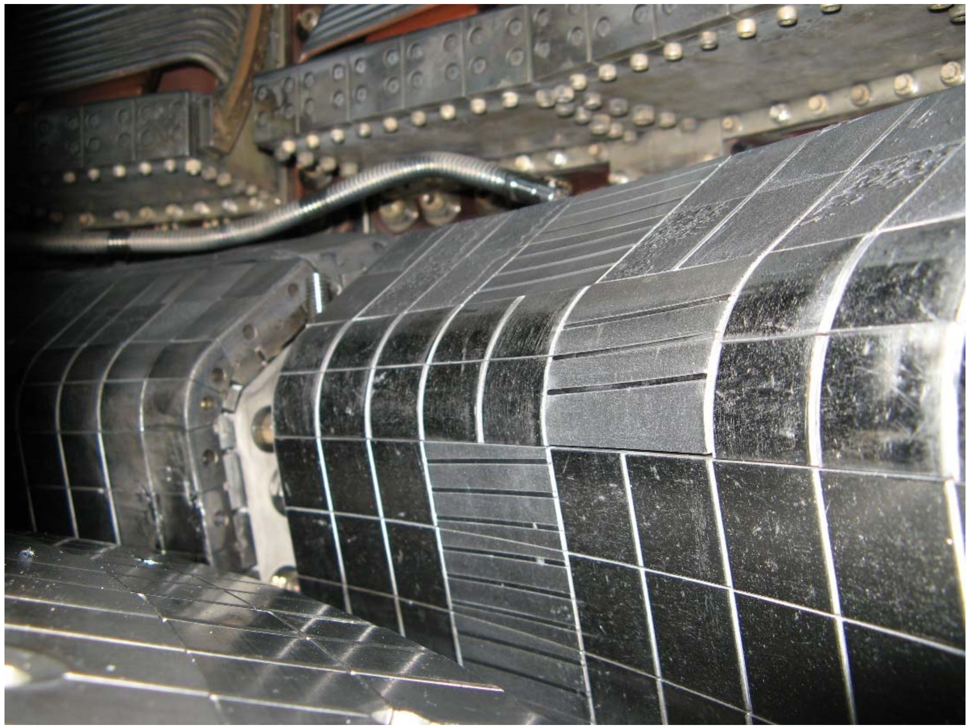

New SOL diagnostic: Langmuir rail probes

- When run in “grounded” mode, the probes appear to the plasma to just be part of the divertor plate surface (almost)
- Current flowing in/out of the probes can be measured while in grounded mode. ***During disruptions, halo currents can be measured.***

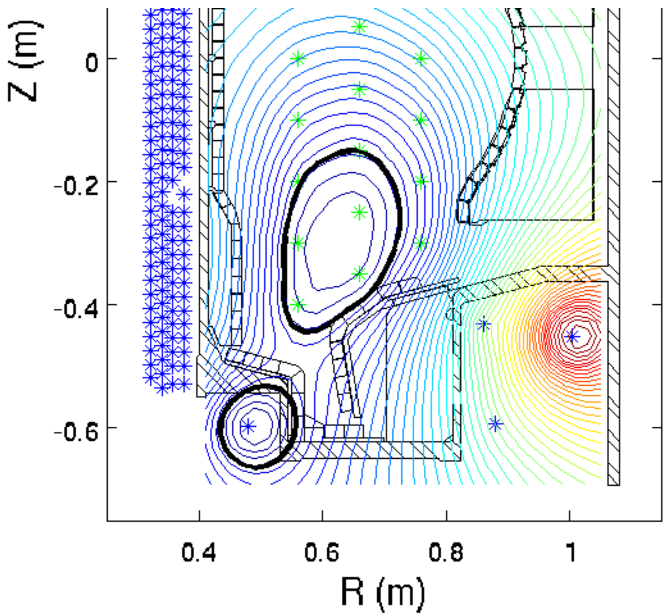

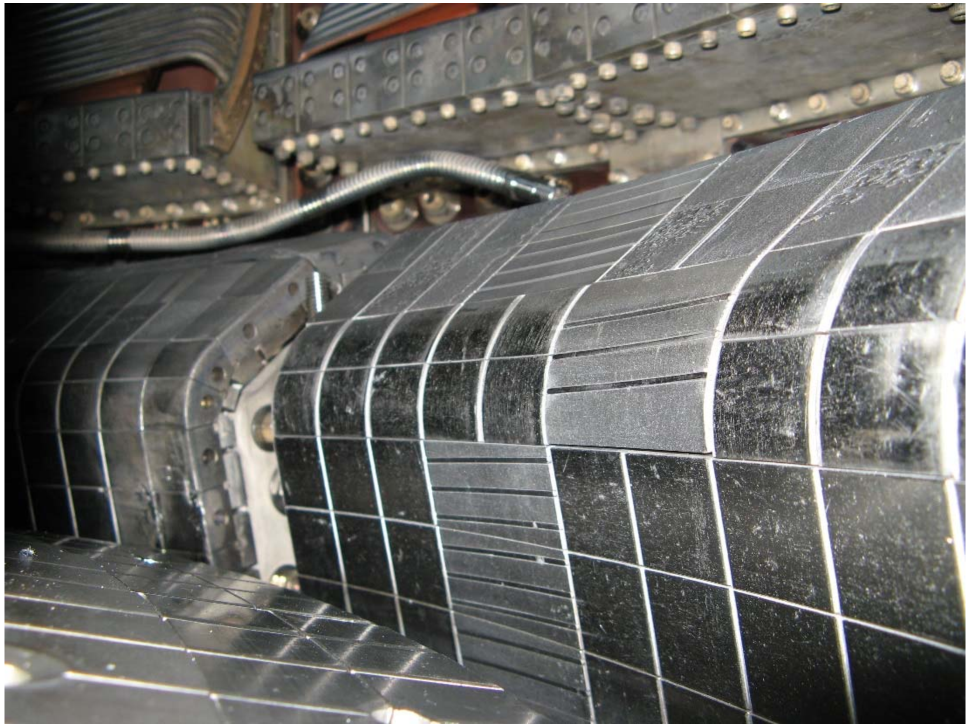

New SOL diagnostic: Langmuir rail probes

- When run in “grounded” mode, the probes appear to the plasma to just be part of the divertor plate surface (almost)
- Current flowing in/out of the probes can be measured while in grounded mode. ***During disruptions, halo currents can be measured.***

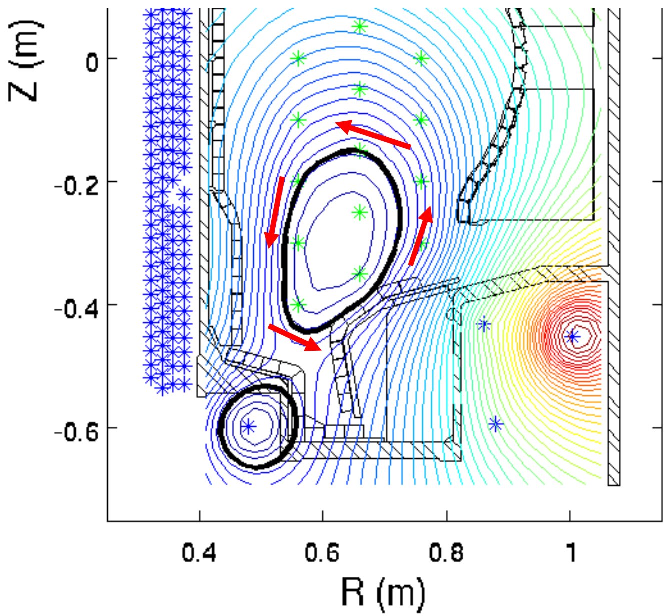

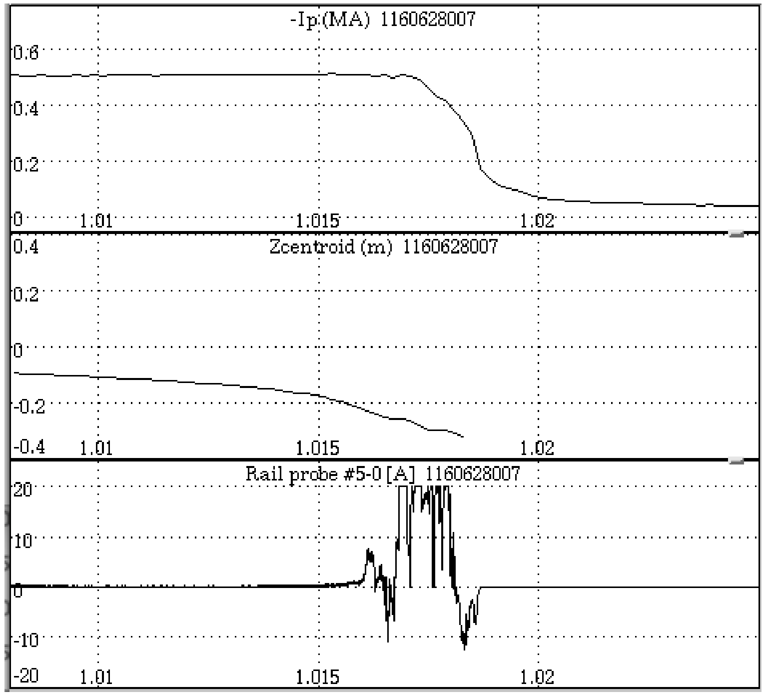

Spatially-resolved halo currents are measured during disruptions

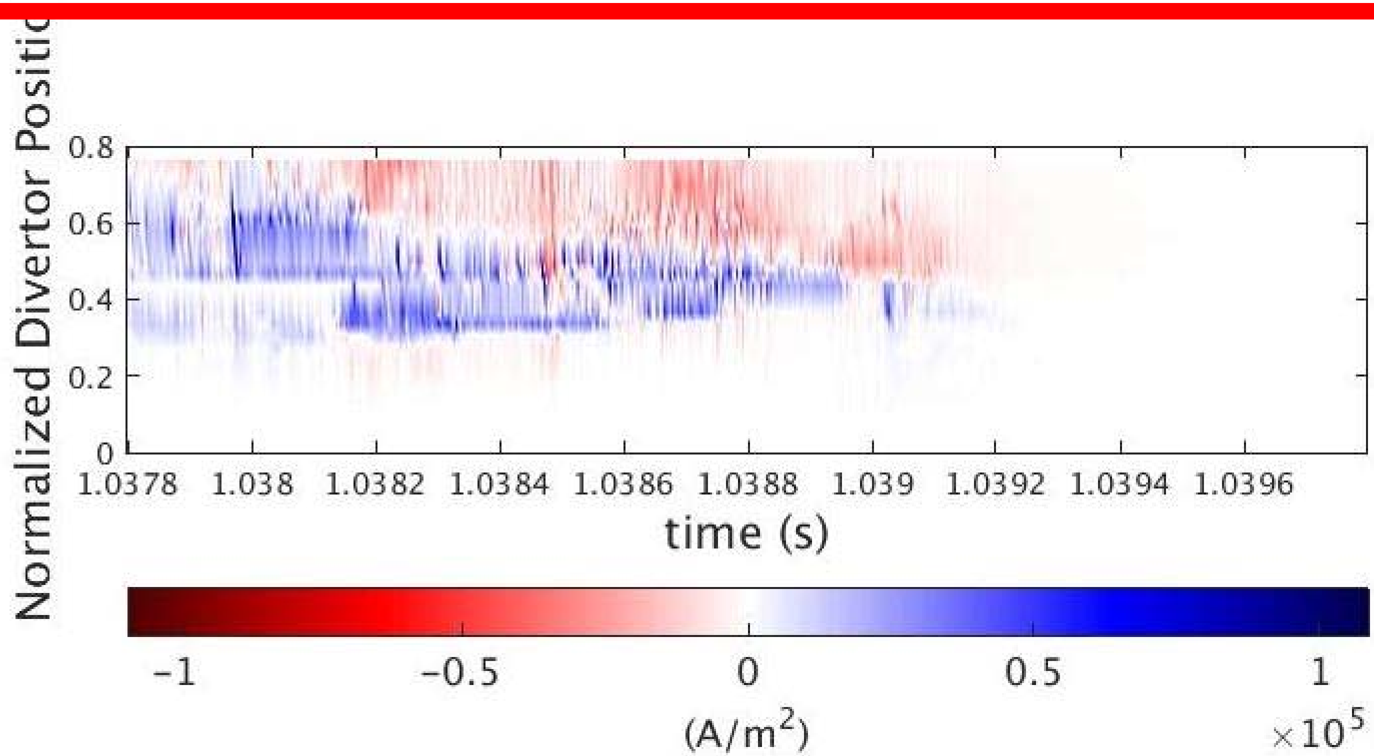

Division between + and – currents slides down the divertor face during the current quench

Spatially-resolved halo currents are measured during disruptions

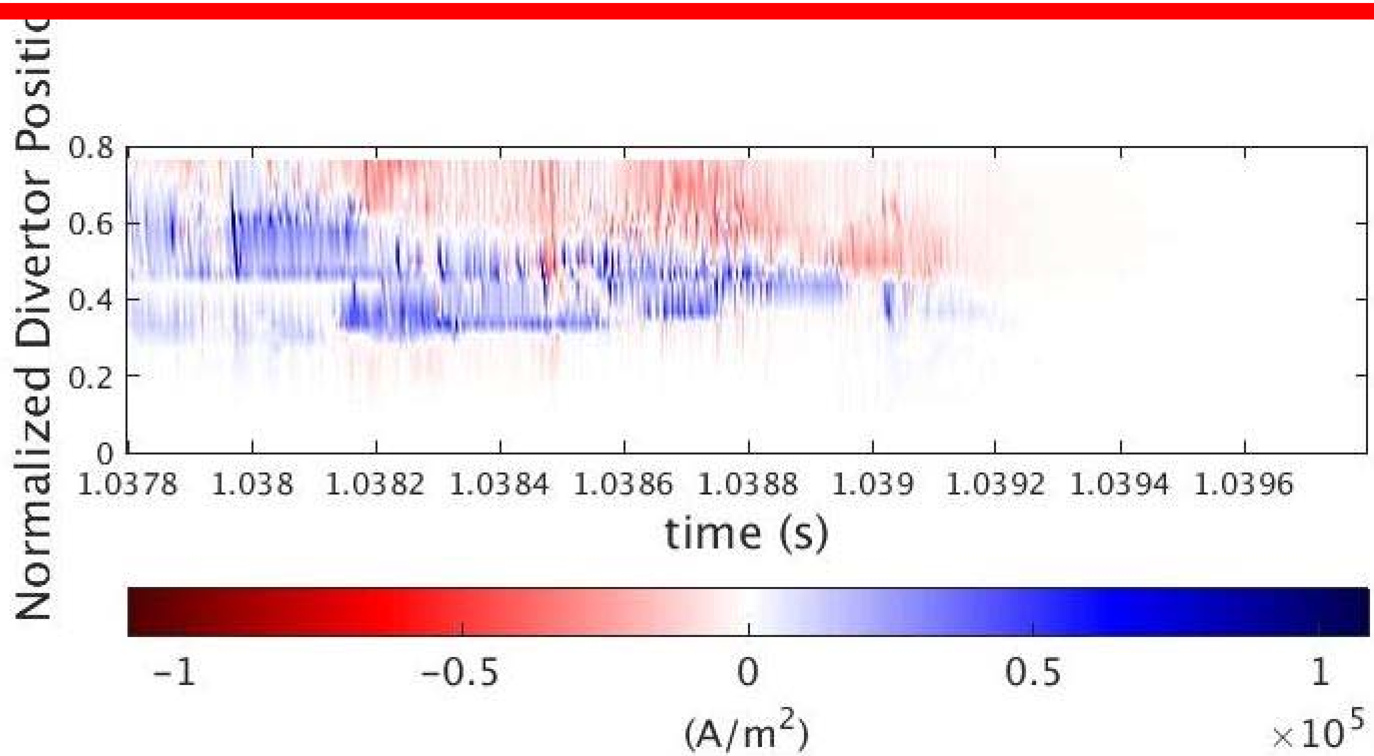

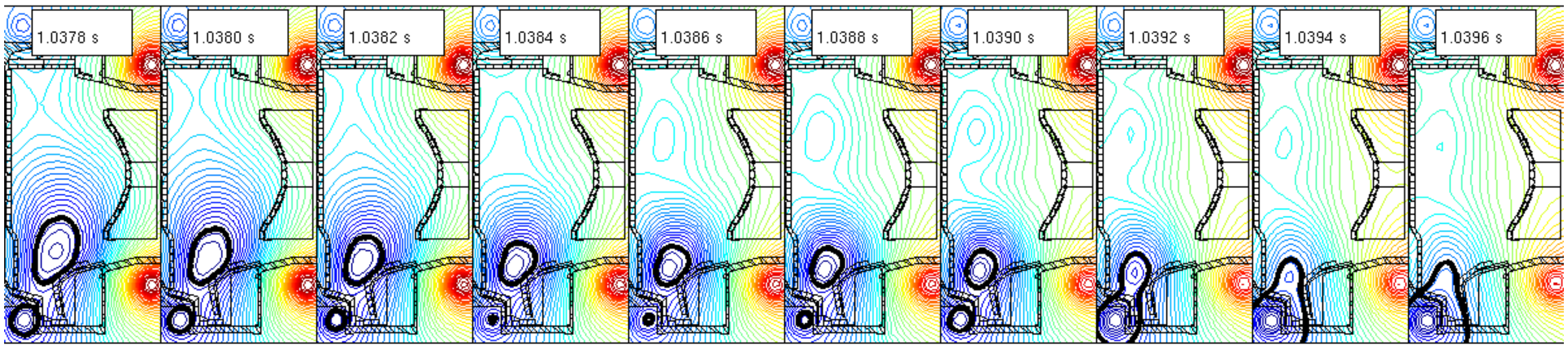

Plasma contact point vs time compared to +/- halo boundary

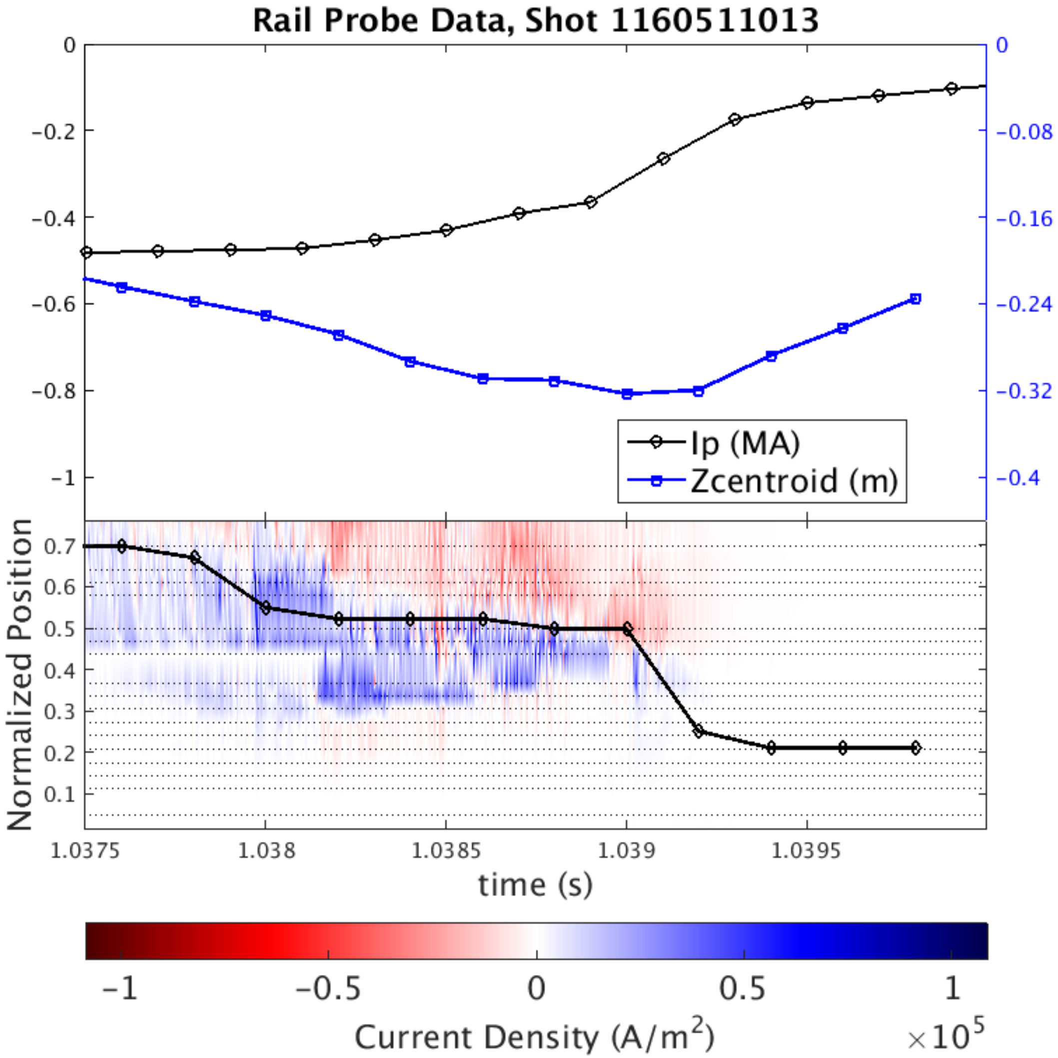

On many disruptions there is good correspondence between contact point and +/- halo boundary vs time

$I_p(t)$ and $Z_c(t)$ are also shown

Contact point is obtained from flux reconstructions using fixed filament model

Plasma contact point vs time compared to +/- halo boundary

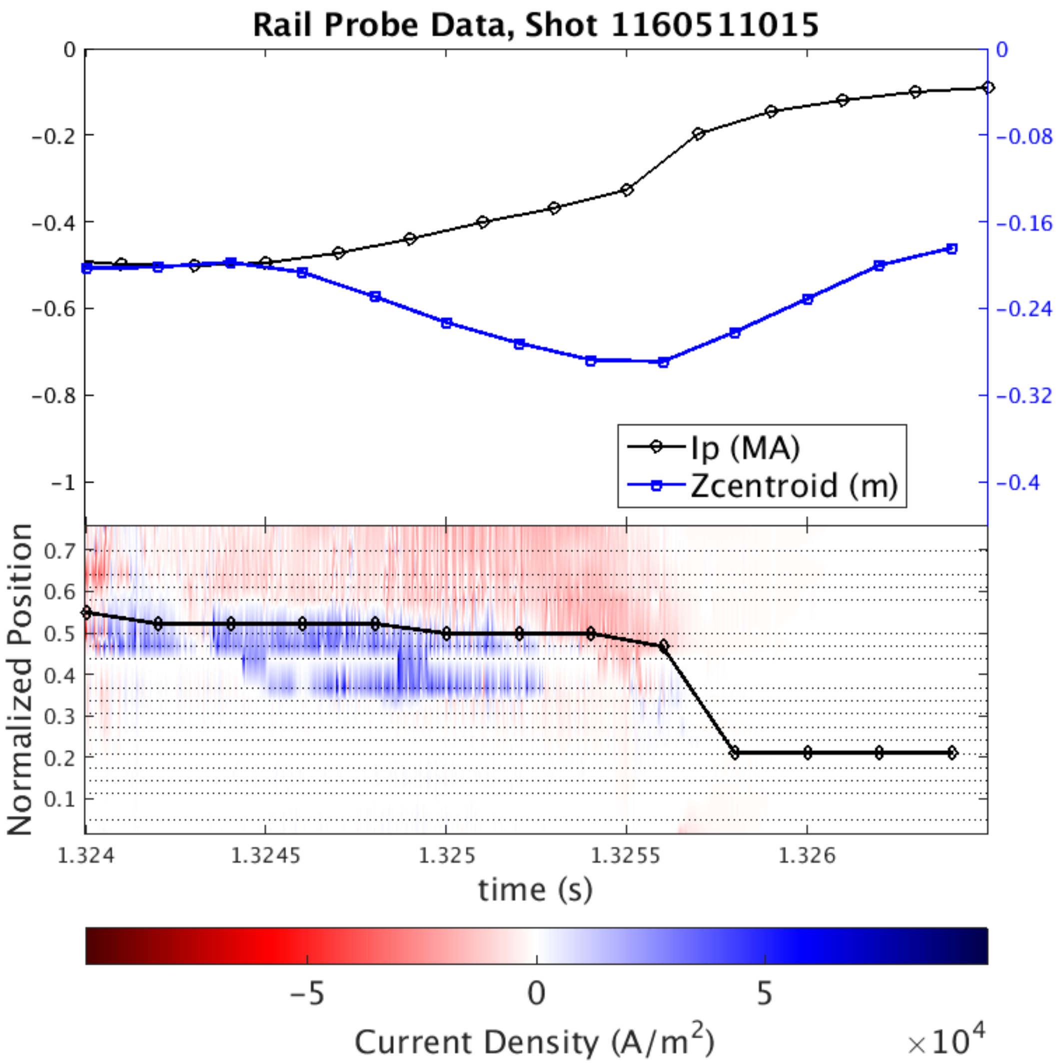

On many disruptions there is good correspondence between contact point and +/- halo boundary vs time

$I_p(t)$ and $Z_c(t)$ are also shown

Contact point is obtained from flux reconstructions using fixed filament model

Resistance of measuring circuit makes a difference

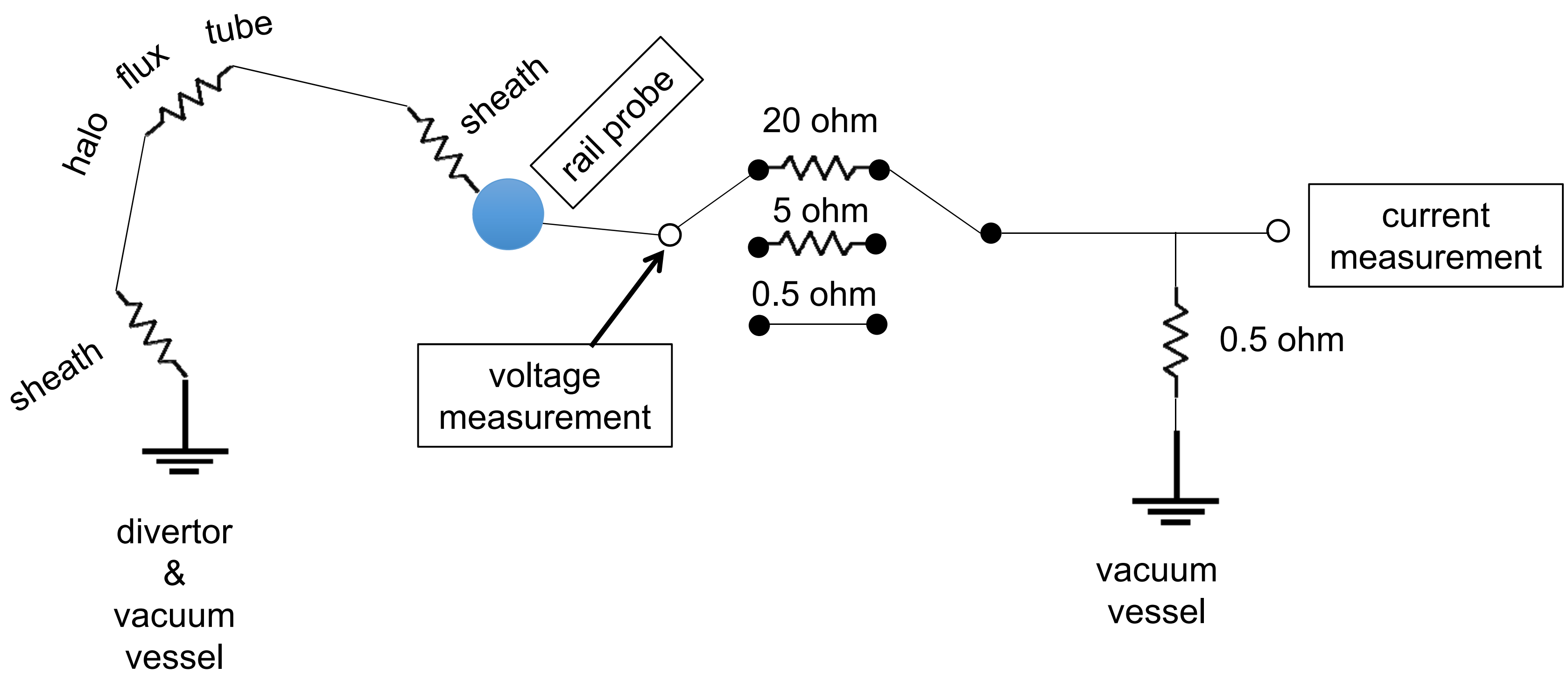

Resistance of measuring circuit makes a difference

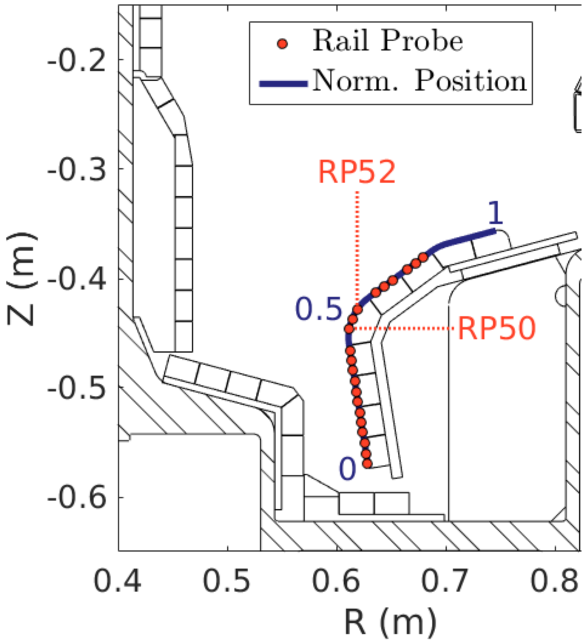

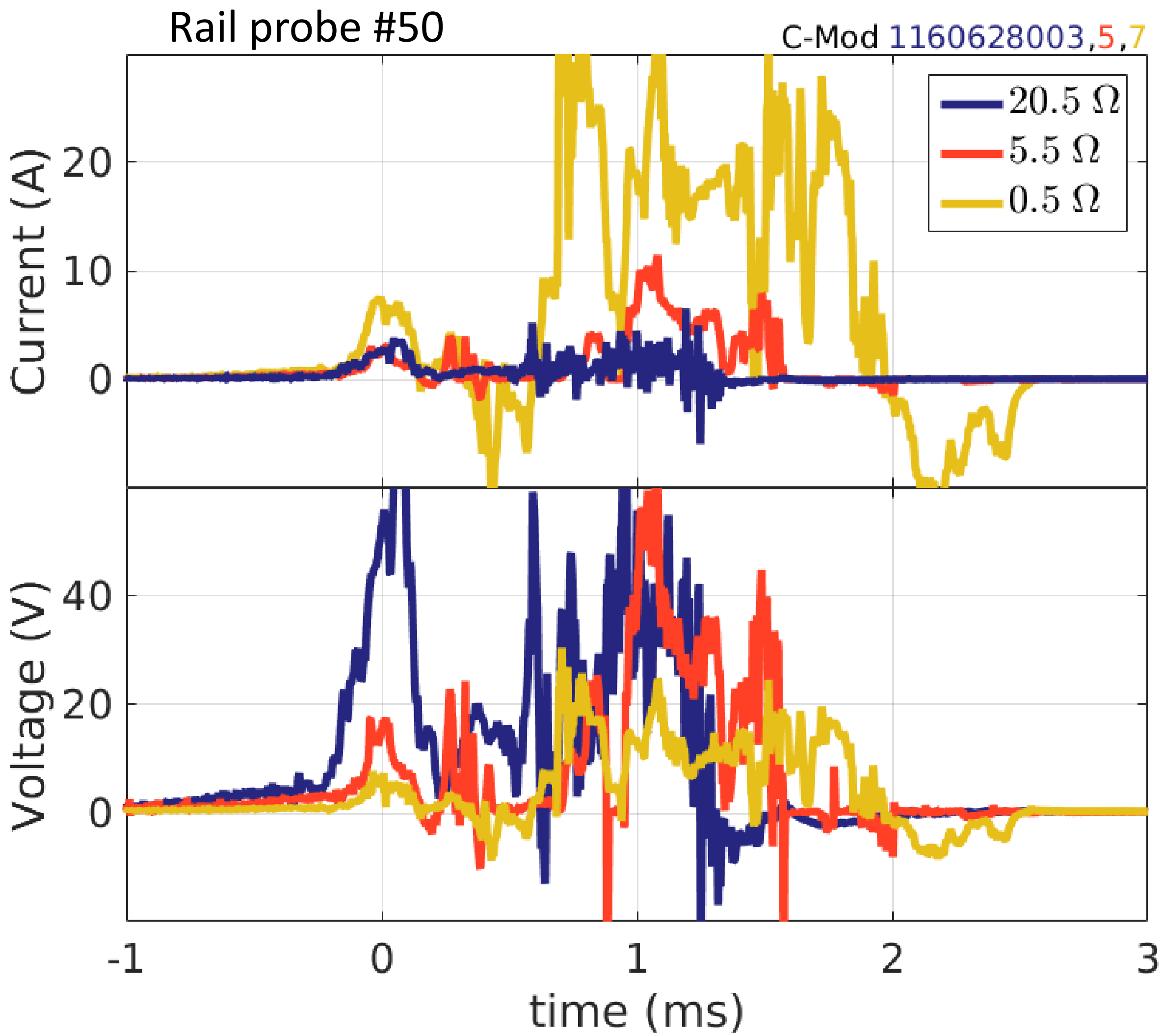

Resistance of measuring circuit makes a difference

Alcator C-Mod

- Halo current measurements with 3 different circuit resistors have been obtained for several of the rail probes, i.e. at several spatial positions in the scrape-off layer
  - At the lowest resistance, we measure total halo current that matches our scaling from 20+ years ago (measured with Rogowski sensors)
- This dependence on the circuit resistor allows us to deduce the actual SOL resistance (Ω), and perhaps even the SOL resistivity profile, if we make the following assumptions:
  1) The disruption current quench generates a voltage, V_{halo}. This voltage drives a current, I_{halo}, that is dependent on the total resistance of the current path.
  2) The V_{halo} generated in each disruption in our set of 6 supposedly identical disruption shots (two shots with each resistor value) is reproducible.

Computing SOL halo resistance

$$V_{halo} = I_{halo}R_{halo} + I_{halo} \times \{20.5, 5.5, 0.5\ \Omega\}$$

2 unknowns: V_{halo} and R_{halo}
6 disruptions with measurements of I_{halo} with 3 different resistors

Method:

1) Select suitable time range for each shot and find average value of I_{halo} (2 A, 6 A, 20 A respectively for rail probe #50)
2) Plot V_{halo} over a range of R_{halo} for each case
3) If curves cross at single point, that is the solution for V_{halo} and R_{halo}

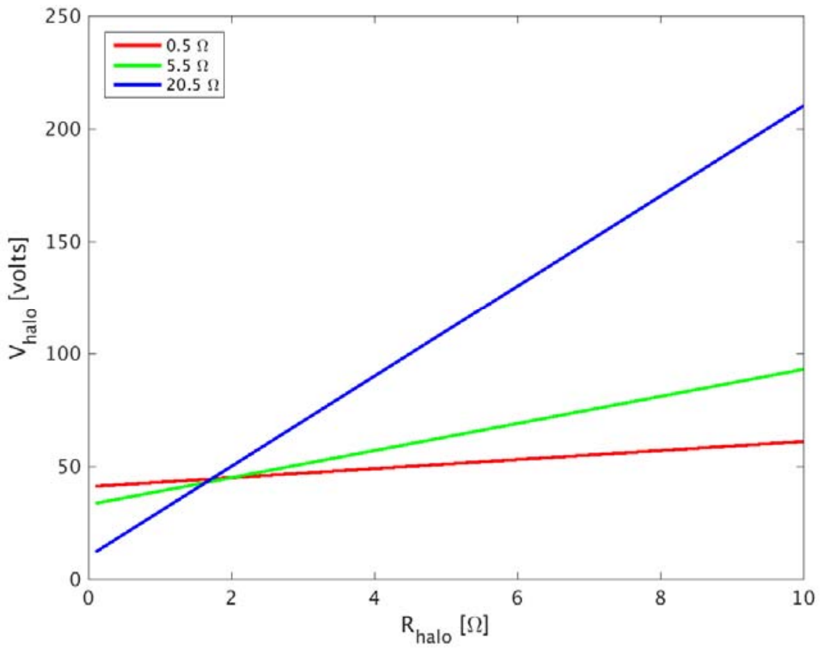

The 3 lines cross at $R_{halo} \sim 1.85\ \Omega$

Summary

- Divertor Langmuir rail probes provide unprecedented poloidally-resolved measurements of disruption halo currents in the SOL
  - Allows detailed comparison of quenching plasma geometry with halo current structure
  - We have also correlated halo currents with edge *q* of quenching plasma
- Dependence on measurement resistors yields information on SOL resistivity and structure
  - Should be useful for modeling
  - Tells us the Z_{eff} of the scrape-off layer during disruption current quenches

Disruption research on Alcator C-Mod

Three topics:

1) High resolution halo current measurements using Langmuir probes
2) Runaway electron synchrotron emission
   - Spectra and energy at 2.7, 5.4, & 7.8 tesla
   - Synthesizing images of RE beams
3) Databases for disruption warning analysis, including applications of machine learning

ITER school on disruptions and control
Aix-en-Provence
2017/03/20-25

PSFC

Alcator C-Mod

Analysis of Runaway Electron Synchrotron Emission in Alcator C-Mod

A. Tinguely[1], R. Granetz[1], M. Hoppe[2], A. Stahl[2], O. Embréus[2]

Thursday, 3 November 2016

Research in Support of ITER

APS DPP, San Jose, CA

[1]Plasma Science and Fusion Center, Massachusetts Institute of Technology, Cambridge, MA

[2]Chalmers University of Technology, Gothenburg, Sweden

Supported by USDoE award DE-FC02-99ER54512.

Runaway electrons may severely damage ITER

Relativistic “Runaway” Electrons (REs):

- Energies > 10 MeV
- Current ≤ 60% of I_p [1]
- In ITER, RE beams of **9 MA**!

RE beam collides with limiter

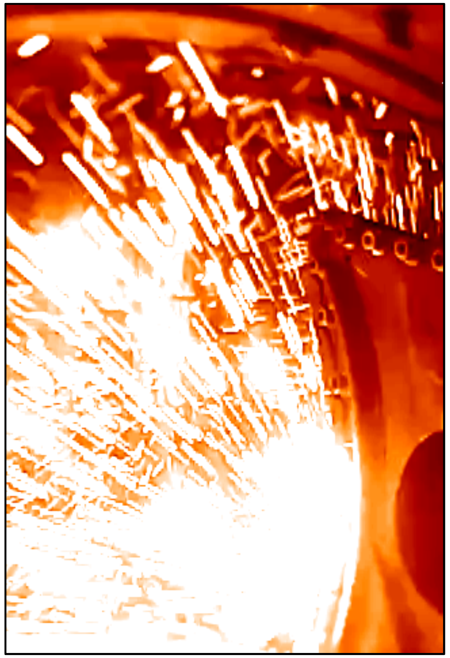

C-Mod 1160824028

[1] V.V. Plyusnin, et al. NF 46, 277-284 (2006).

Runaway electrons may severely damage ITER

Relativistic "Runaway" Electrons (REs):

- Energies > 10 MeV
- Current $\leq 60\%$ of I_p [1]
- In ITER, RE beams of **9 MA**!

Collisional drag O(1)

$$\frac{dp}{dt} = \mathbf{F_E} + \mathbf{F_C}\left(\frac{\mathbf{n}}{\mathbf{p^2}}\right) + \mathbf{F_{ALD}}(\mathbf{p_\parallel}, \mathbf{p_\perp}, \mathbf{B})$$

Electric force O(5-10) [2]

Radiation reaction O(3-15)

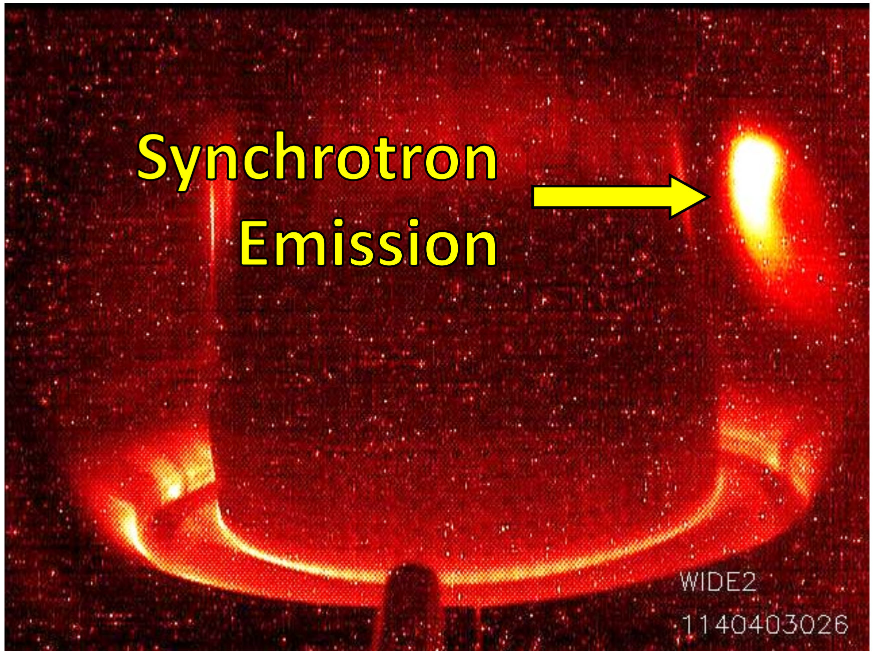

[1] V.V. Plyusnin, et al. NF 46, 277-284 (2006).
[2] R.S. Granetz, et al. PoP 21, 072506 (2014).

Absolutely-calibrated visible/NIR spectrometers (~300-1000 nm) measure SE on C-Mod.

	C-Mod	ITER
B_{tor} (T)	5.4 (2 – 8)	5.3
$\bar{n}_e$ (10^{20} m^{-3})	1 (0.2 – 4)	1.0

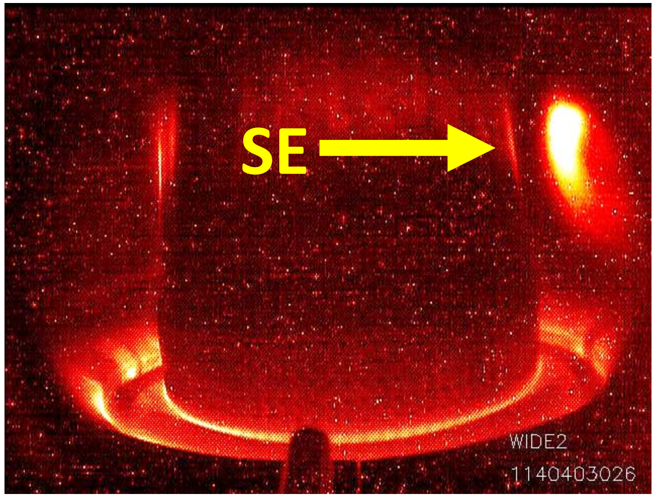

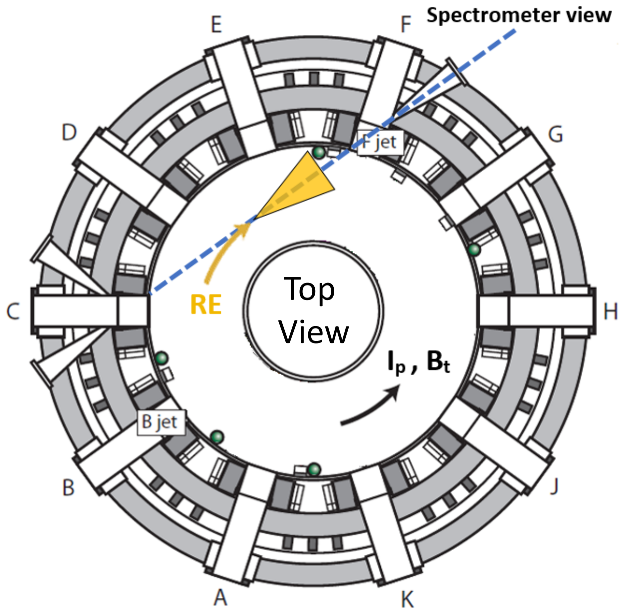

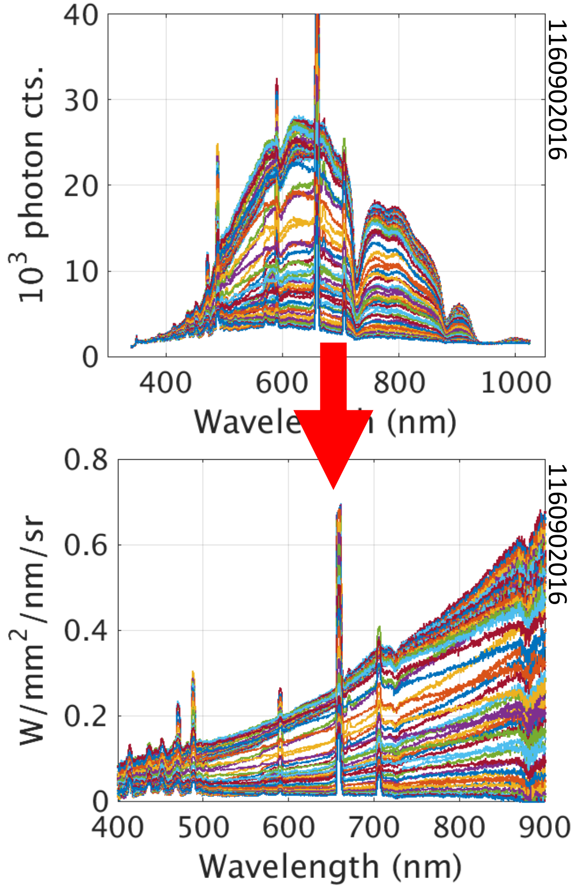

Does synchrotron emission limit the maximum energy of REs?

Consider an electron with energy E = 40 MeV and pitch = 0.1 in three different magnetic fields.

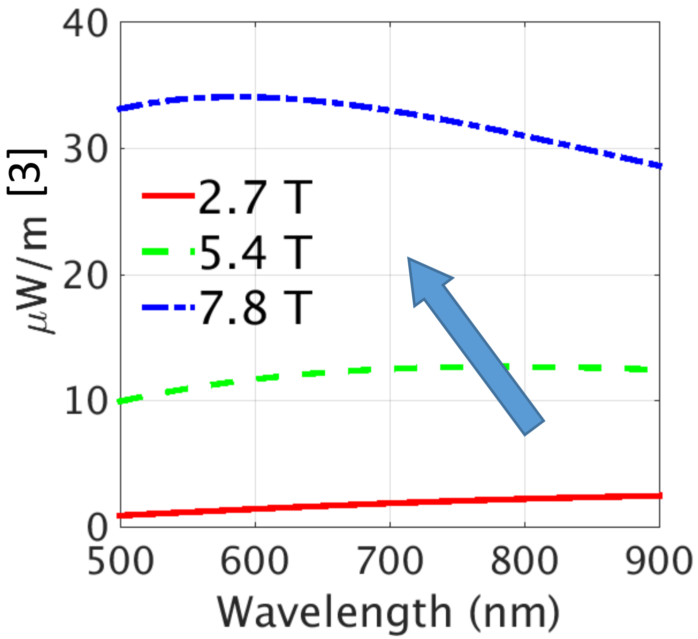

[3] I.M. Pankratov. Plasma Phys. Reports 25, 2 (1999).

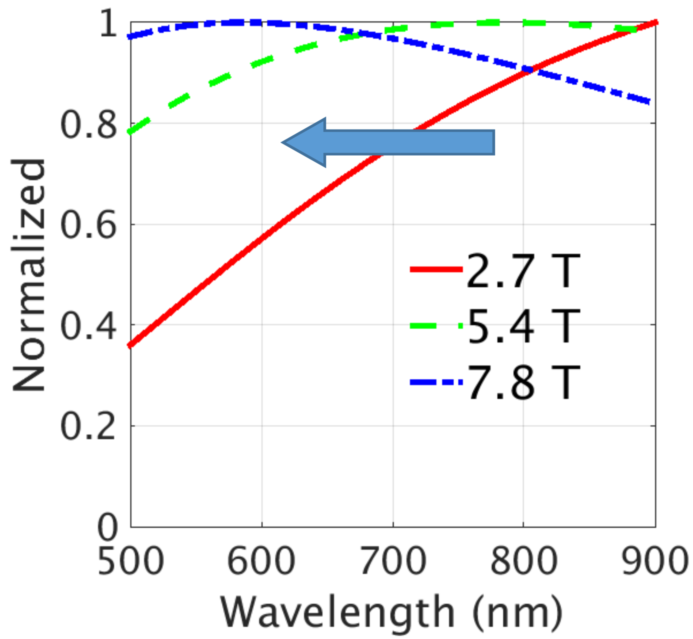

Absolutely-calibrated visible/NIR spectrometers measure synchrotron emission on C-Mod

- RE densities are difficult to reproduce, so we are not interested in the absolute amplitude.
- Instead, we are interested in the spectral shape.

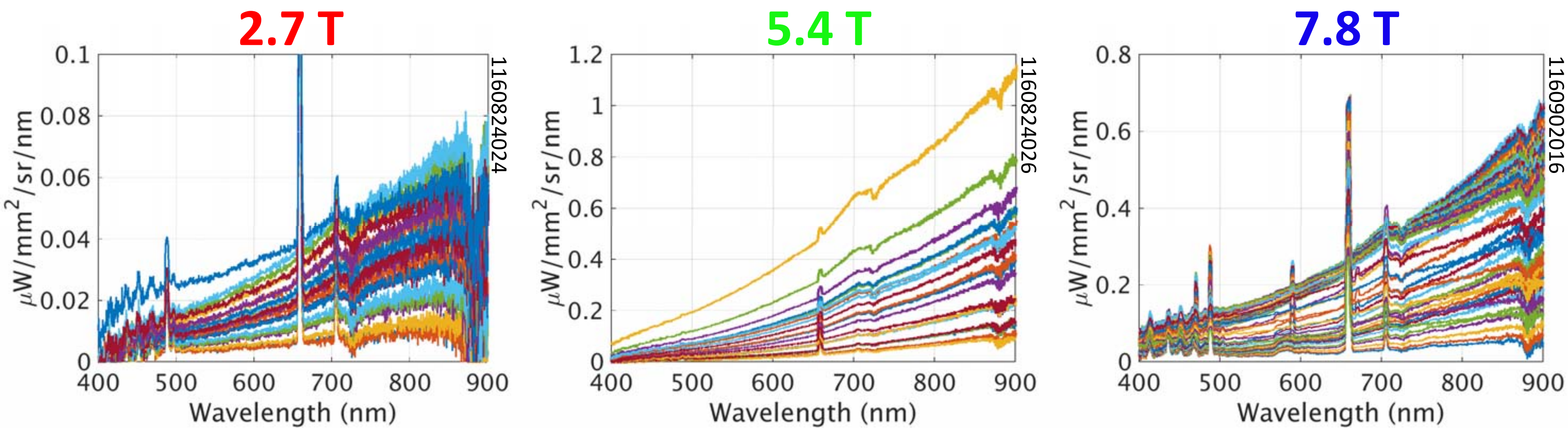

Absolutely-calibrated visible/NIR spectrometers measure synchrotron emission on C-Mod

- Select one time-slice near maximum emission during steady plasma parameters.
- Take the ratio of two spectra and normalize.

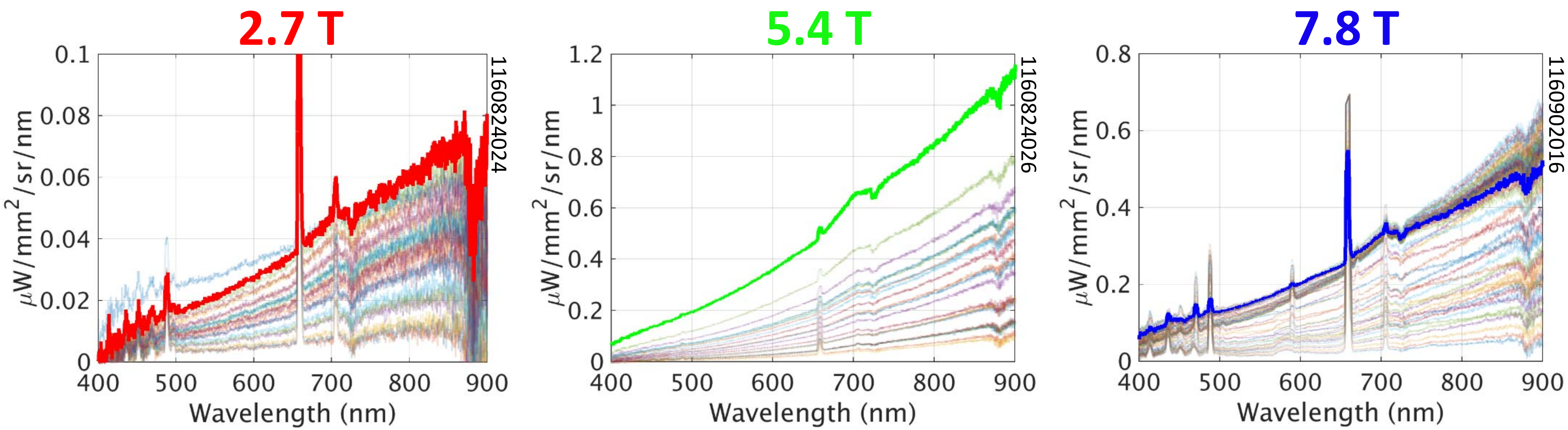

Compare synchrotron emission at three magnetic fields

*Relative to the **reference** spectra

Positive slope

- More brightness at longer wavelengths
- Shifted toward the **red**

Negative slope

- More brightness at shorter wavelengths
- Shifted toward the **blue**

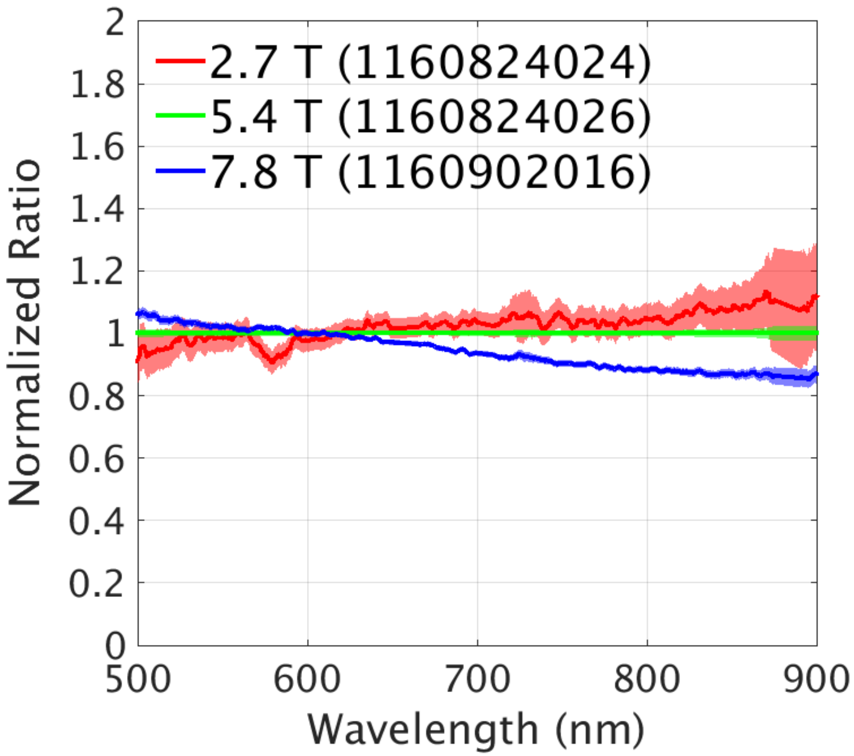

Compare synchrotron emission at three magnetic fields

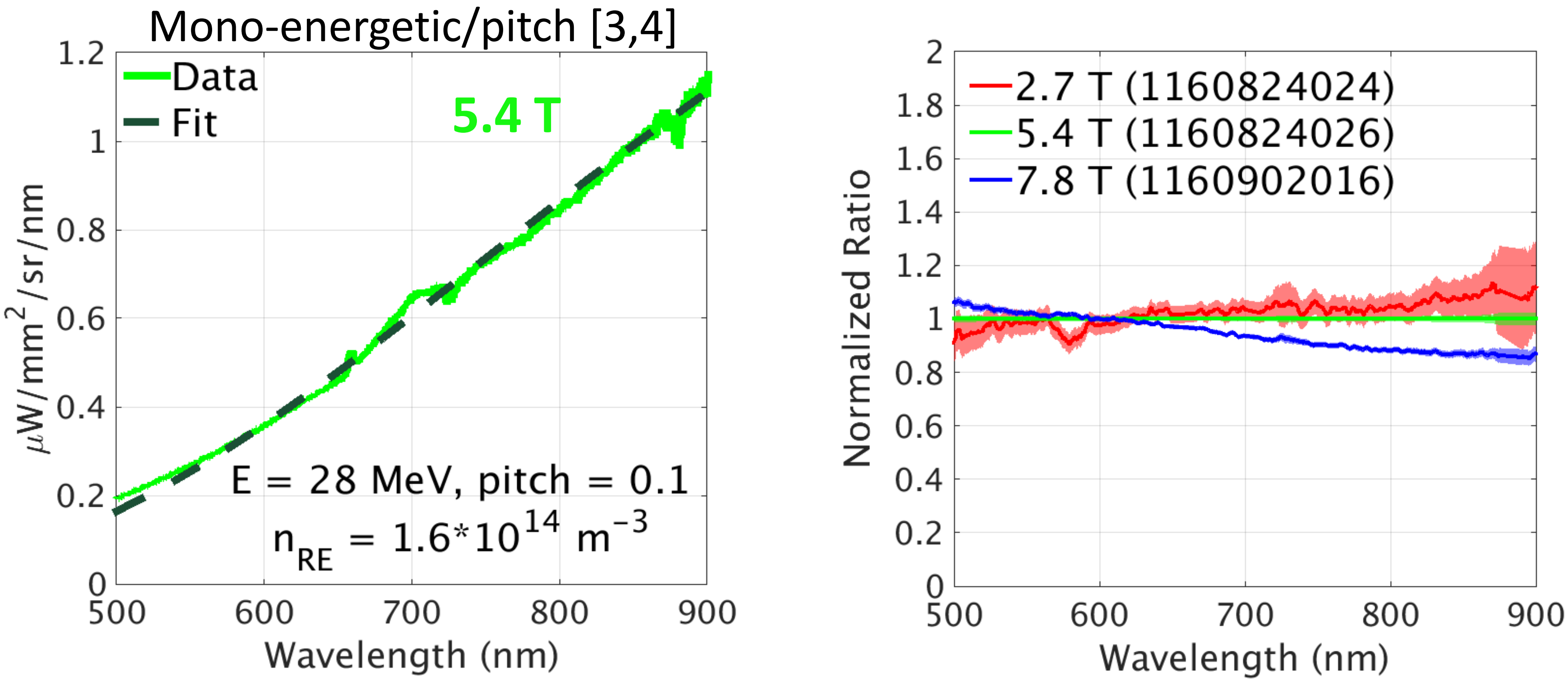

[3] I.M. Pankratov. Plasma Phys. Reports 25, 2 (1999).
[4] J.H. Yu, et al. PoP 20, 042133 (2013).

Compare synchrotron emission at three magnetic fields

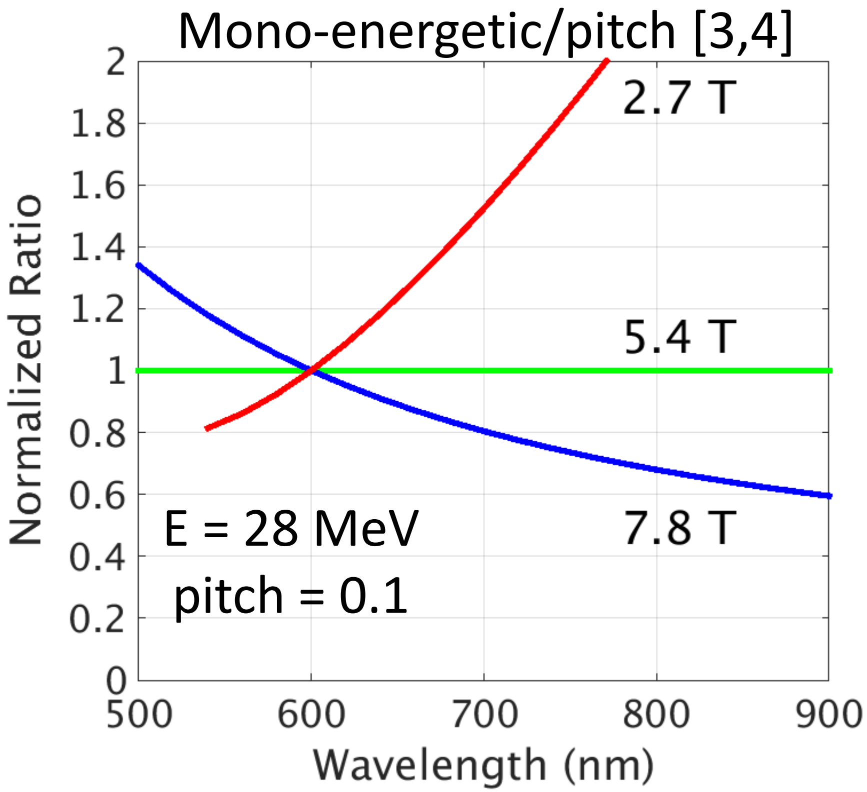

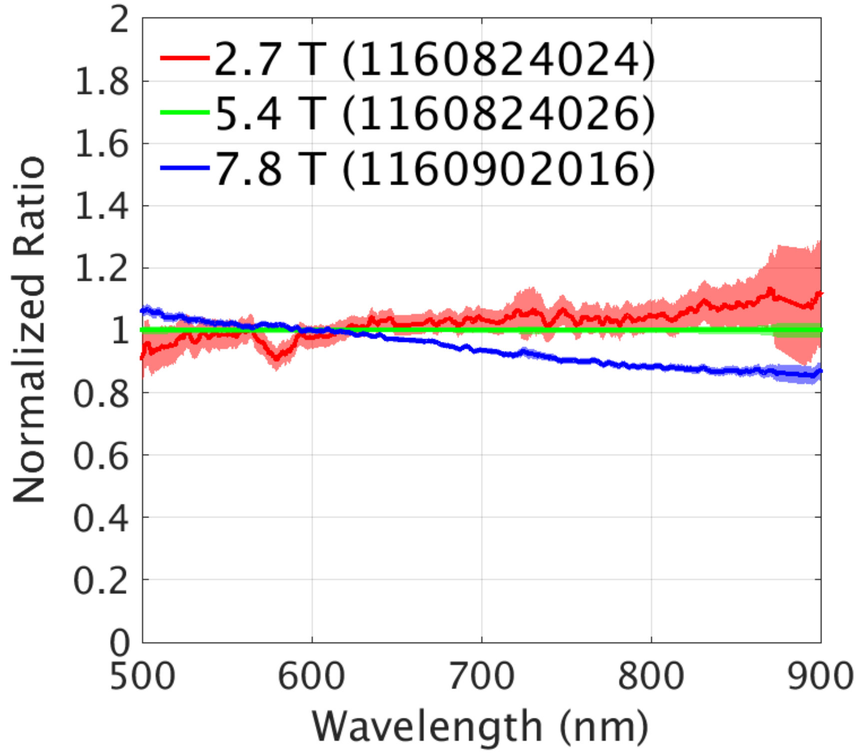

[3] I.M. Pankratov. Plasma Phys. Reports 25, 2 (1999).
[4] J.H. Yu, et al. PoP 20, 042133 (2013).

Compare synchrotron emission at three magnetic fields

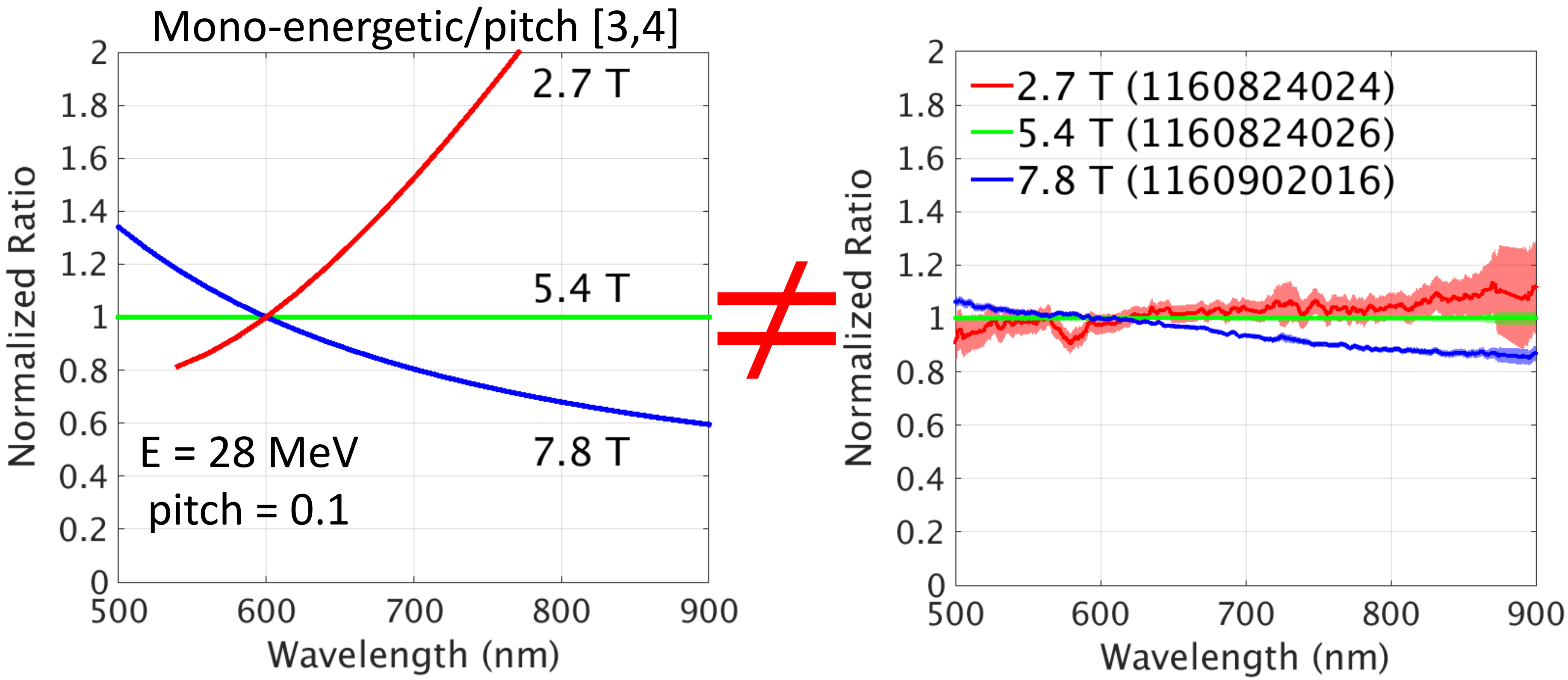

[3] I.M. Pankratov. Plasma Phys. Reports 25, 2 (1999).
[4] J.H. Yu, et al. PoP 20, 042133 (2013).

Decreasing RE **energy** decreases synchrotron emission amplitude and shifts toward the red

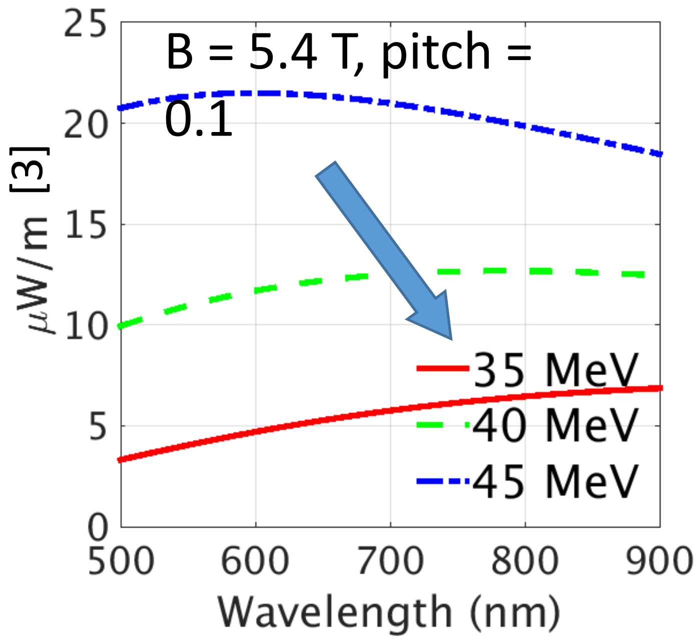

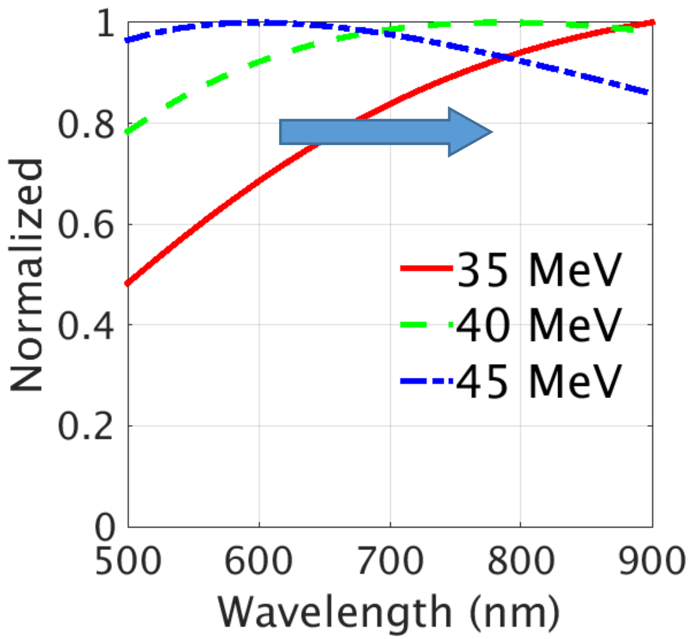

→ To keep the brightness the same, an increase in magnetic field requires a decrease in energy.

[3] I.M. Pankratov. Plasma Phys. Reports 25, 2 (1999).

Synchrotron emission limits the mono-energetic RE energy

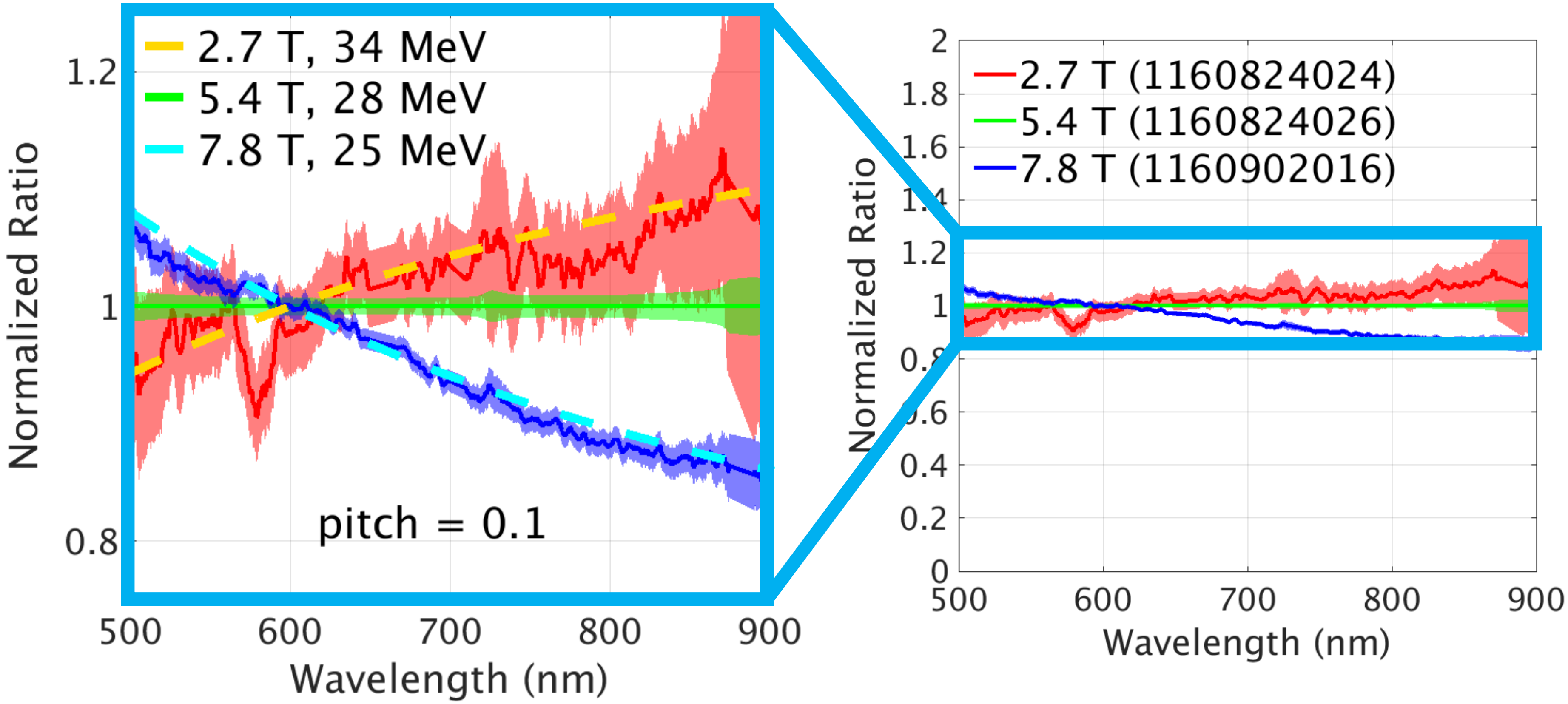

Summary of Results

- Per particle, synchrotron emission increases and shifts toward shorter wavelengths with increasing magnetic field and energy (for fixed pitch).

- Measured synchrotron brightnesses at three magnetic fields (2.7 T, 5.4 T, and 7.8 T) have similar spectral shapes.

- Assuming a mono-energetic RE beam at a fixed pitch, an increase in synchrotron emission per particle (from an increase in magnetic field) reduces the energy.

  → Synchrotron emission is limiting the energy of REs.

Preliminary results from synthetic diagnostic SOFT [5] show good agreement with experiment

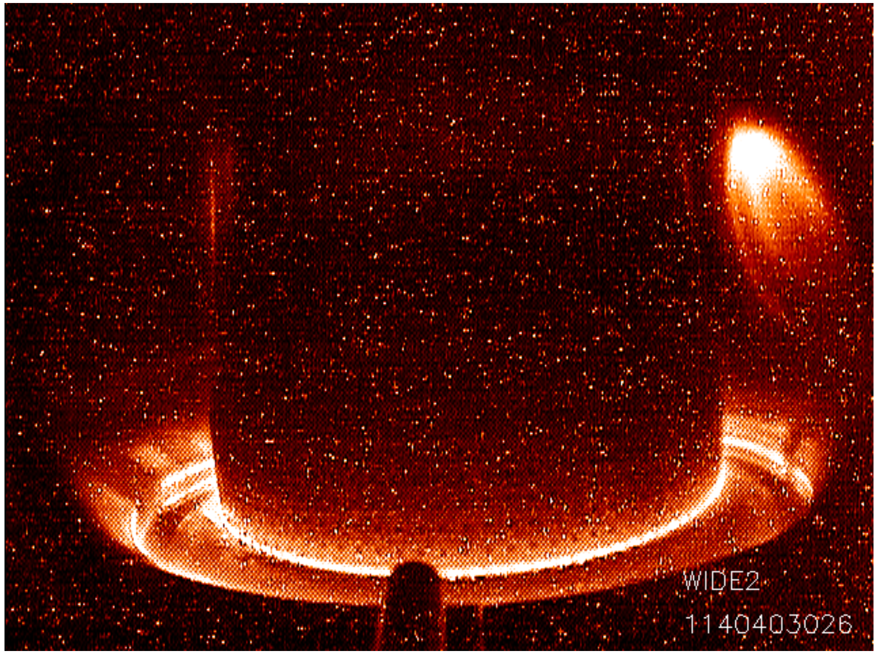

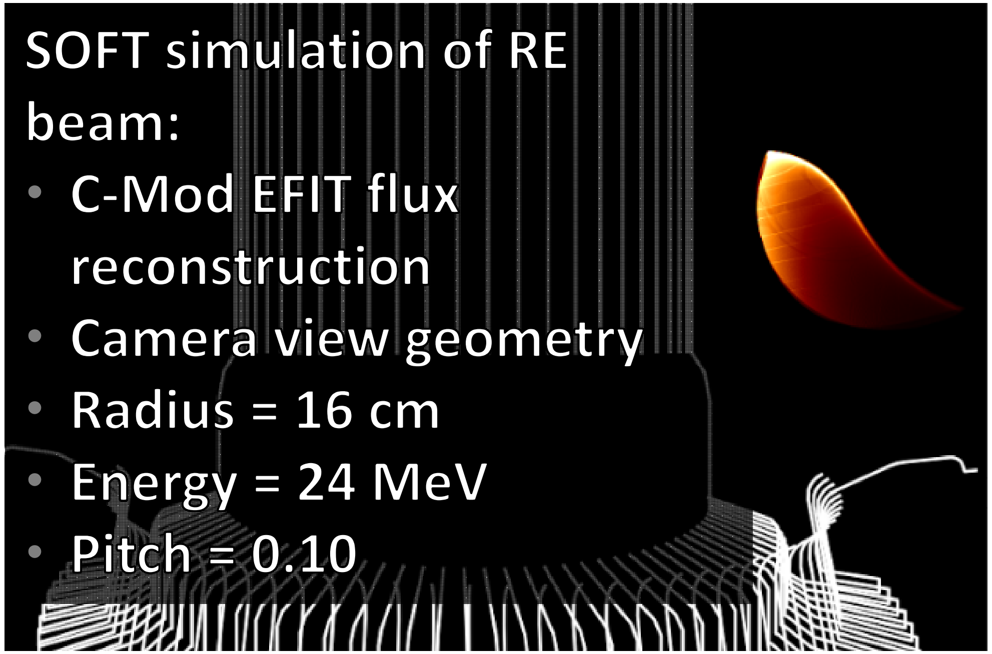

SOFT simulation of RE beam:
- C-Mod EFIT flux reconstruction
- Camera view geometry
- Radius = 16 cm
- Energy = 24 MeV
- Pitch = 0.10

[5] Correspondence with M. Hoppe and the Chalmers Plasma Physics Group (2016).

References

[1] V.V. Plyusnin, et al. NF 46, 277-284 (2006).

[2] R.S. Granetz, et al. PoP 21, 072506 (2014).

[3] I.M. Pankratov. Plasma Phys. Reports 25, 2 (1999).

[4] J.H. Yu, et al. PoP 20, 042133 (2013).

[5] M. Hoppe, Chalmers Plasma Physics Group (private communication, 2016).

Disruption research on Alcator C-Mod

Three topics:

1) High resolution halo current measurements using Langmuir probes
2) Runaway electron synchrotron emission
   - Spectra and energy at 2.7, 5.4, & 7.8 tesla
   - Synthesizing images of RE beams
3) Databases for disruption warning analysis, including applications of machine learning

ITER school on disruptions and control
Aix-en-Provence
2017/03/20-25

Developing Disruption Warning Algorithms Using Large Databases on Alcator C-Mod, EAST, and DIII-D

R. Granetz, C. Rea, A. Tinguely

MIT Plasma Science and Fusion Center, Cambridge, MA, US

Why Large Databases Are Useful for Developing Disruption Warning Algorithms

We want to answer the following types of questions:

- Which parameters are correlated with the approach of a disruption? What are their threshold levels vs number of missed disruptions *and* number of false positives?
- What is the warning time vs threshold level?
- Do the details depend on whether the disruption occurs during flattop, rampdown, or rampup?
- Are there combinations of parameters that are useful?
- ***Are the same parameters useful on different tokamaks?***

Additionally, we desire a disruption warning algorithm that works in near real-time, embedded in the plasma control system

➢ Therefore, the only parameters in our databases are those that, in principle, can be available in near real-time.

The Databases We Are Constructing

We have created databases consisting of candidate parameters sampled at many times during disruptive ***and*** non-disruptive shots on several tokamaks:

C-Mod 2015 campaign (~2000 shots; > 165,000 time slices)
EAST 2015 campaign (~3000 shots; > 117,000 time slices)
DIII-D 2015 campaign (~2100 shots; > 500,000 time slices)

- Non-uniform time slice sampling:
  - Flattop, rampdown, rampup can have different sampling rates
  - **Additional slices at much higher sampling frequency for a fixed period of time before a disruption**
- SQL, using standard queries with MATLAB, IDL, Python,
- Potentially could be processed using "machine learning" algorithms such as deep neural networks, support vector machines(SVM), random forests, …

Comparisons of several possible disruption warning indicators on C-Mod and EAST

In this poster we will compare 3 plasma parameters that are commonly associated with impending disruptions:

- **Loop voltage** – Increasing impurity content and/or MHD instabilities can increase plasma resistivity, causing an increase in V_{loop}, and possibly leading to a disruption
- **P_{rad} fraction** – An increase in P_{rad}/P_{input} may provide an early warning of an impending thermal collapse due to impurity radiation
- **I_p error** – Difference between the actual plasma current and the pre-programmed plasma current. This can be due to an increase in resistivity caused by impurities or MHD, possibly leading to a disruption

Important details:

- All data in the following plots are taken from the **flattop** portion of the discharge. (Our databases have data from rampup and rampdown as well, but here we concentrate on the flattop only.)
- All disruptions in the following plots occur during flattop
- Both disruptive and non-disruptive discharges are analyzed.
  - Disruptive discharges give prediction success rate
  - Non-disruptive discharges give false positive rate
- ***It is absolutely imperative to avoid processing signals with non-causal filtering.*** This can introduce post-disruption effects into pre-disruption data. Particular care must be taken with P_{rad} and V_{loop}

Parameter: Loop voltage
Tokamak: EAST

Non-disruptions

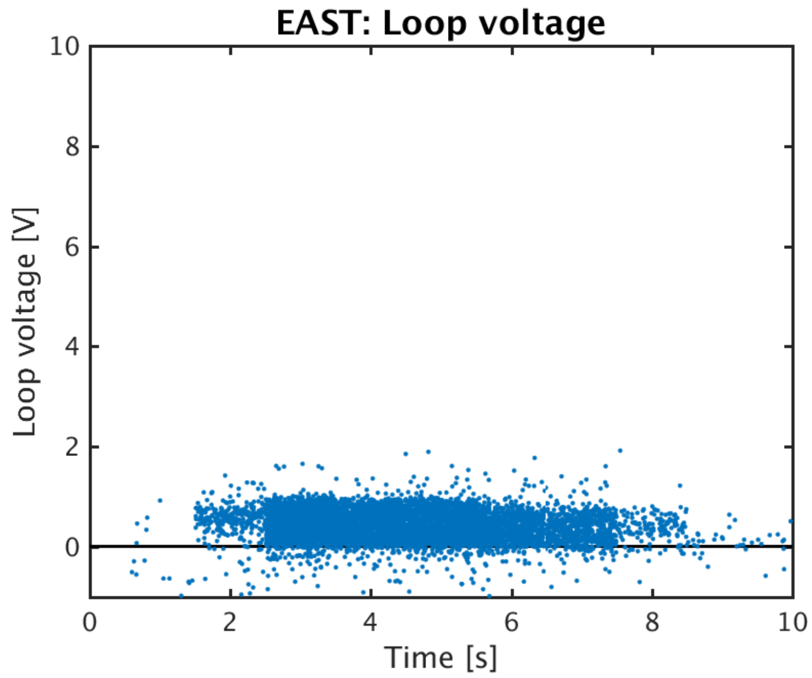

Disruptions

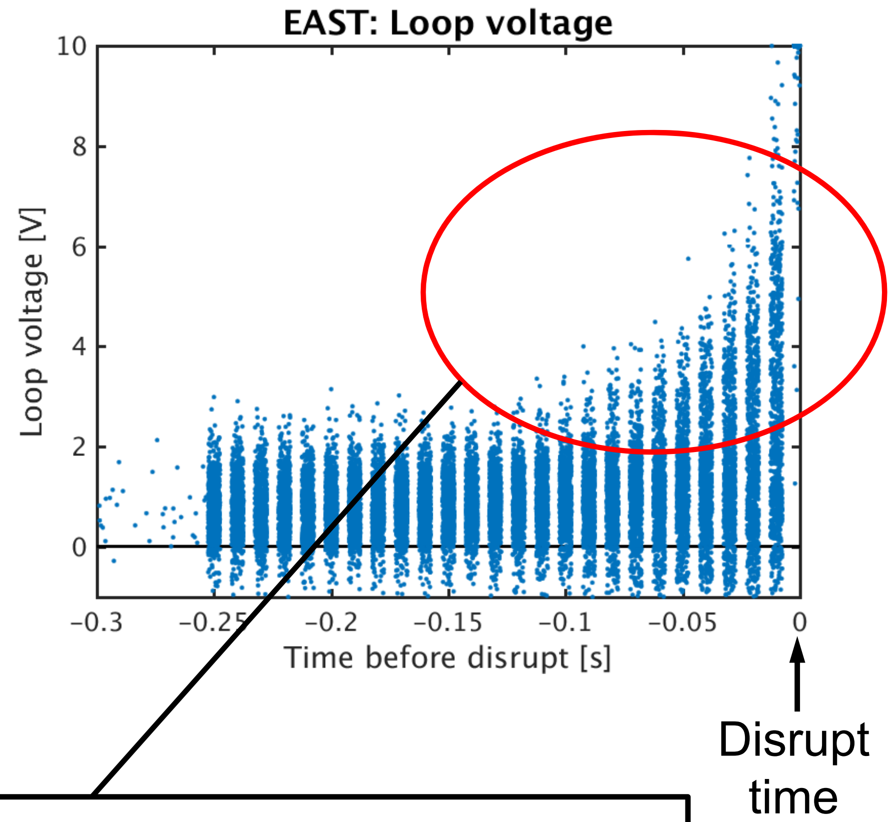

A significant number of loop voltage values increase during the ~100 ms before disruptions occur

Parameter: Loop voltage
Tokamak: EAST

Non-disruptions	Disruptions

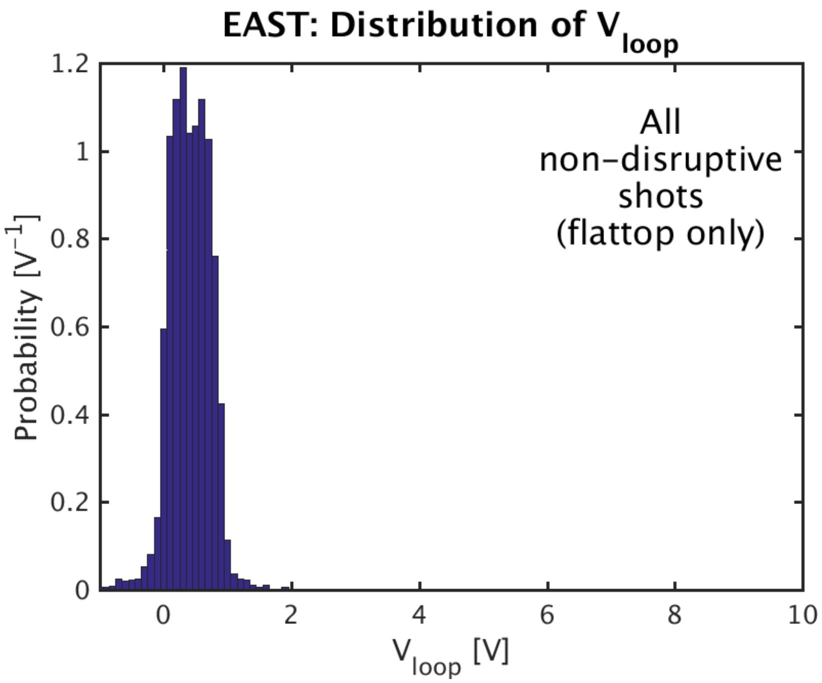

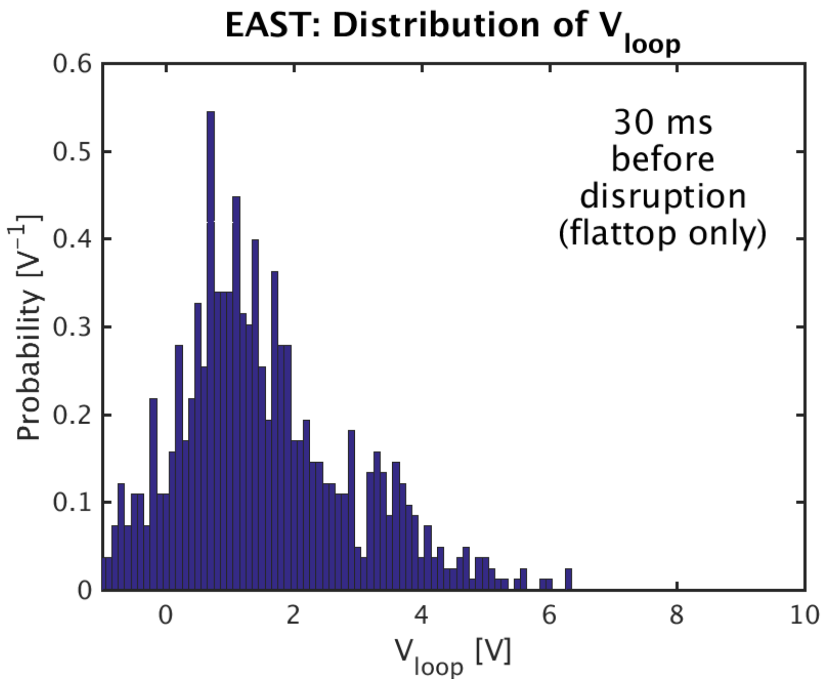

If we declare: ($V_{loop} \geq 1.5$ or $V_{loop} \leq -0.7$) is threshold for disrupt:
- 47.8% of disruptions are predicted with ≥ 30 ms warning time
  - 0.7% false positive rate

Parameter: Loop voltage
Tokamak: C-Mod

Non-disruptions

Disruptions

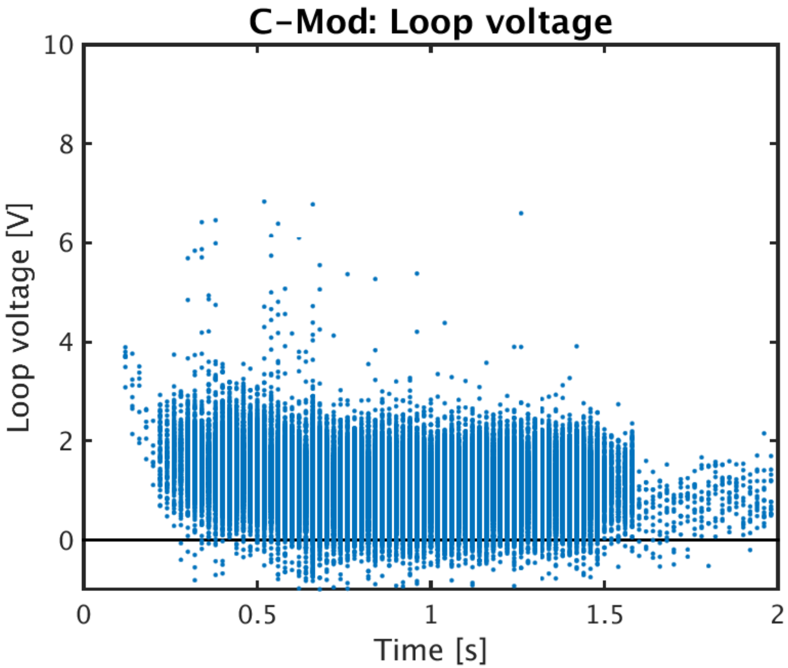

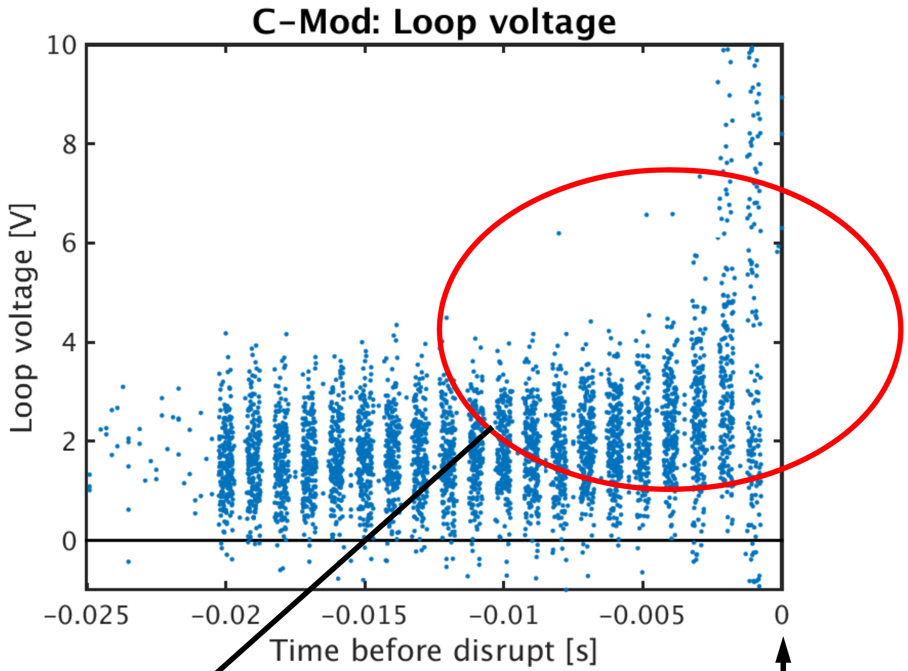

Disrupt time

Loop voltage values do not increase until < 5 ms before disruptions occur

Parameter: Loop voltage
Tokamak: C-Mod

Non-disruptions

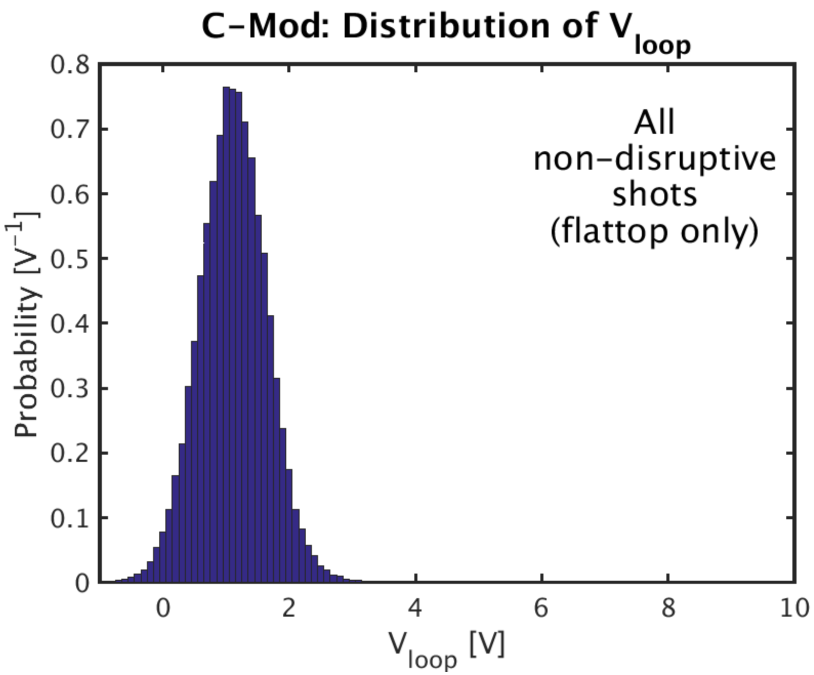

Disruptions

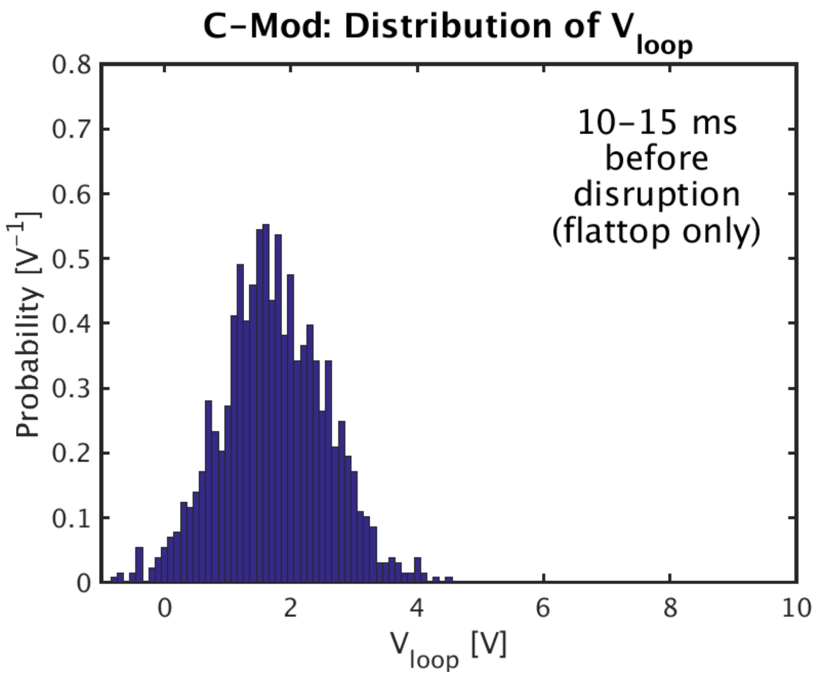

If we declare: ($V_{loop} \geq 2.9$ or $V_{loop} \leq -0.7$) is threshold for disrupt:

9.2% of disruptions are predicted with ≥ 10 ms warning time

0.6% false positive rate

Parameter: P_{rad} fraction
Tokamak: EAST

Non-disruptions

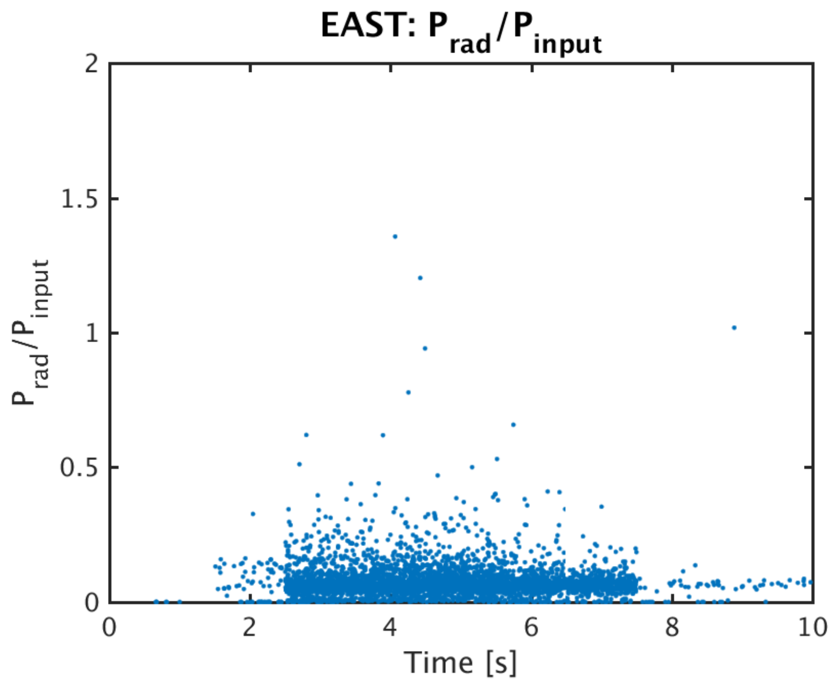

Disruptions

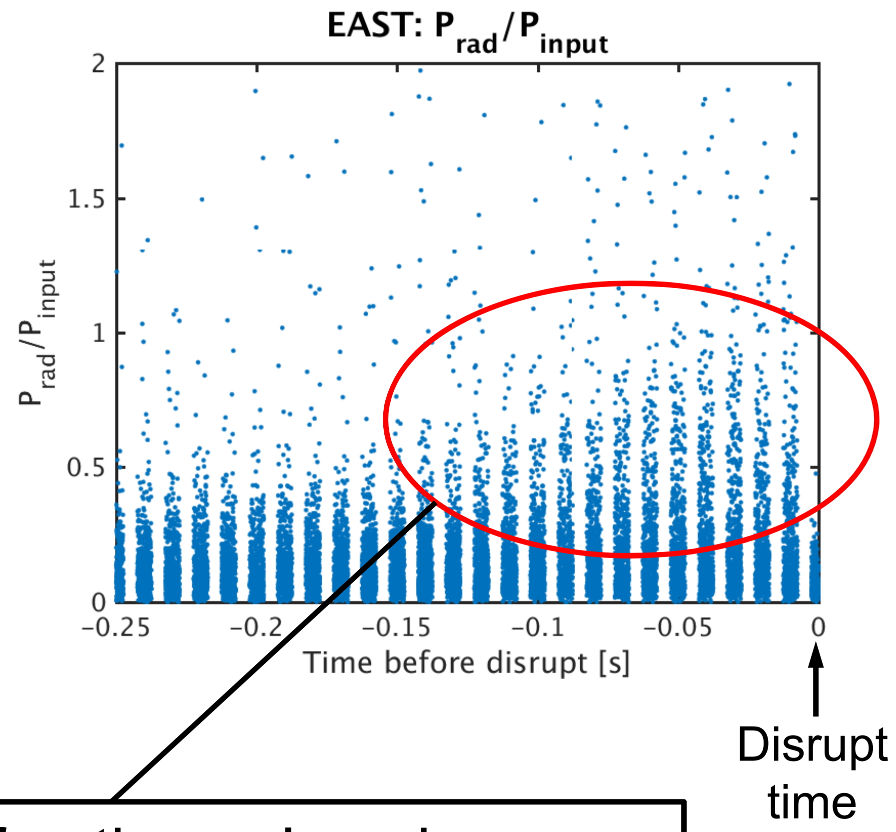

A significant number of P_{rad} fraction values increase during the ~150 ms before disruptions occur

Parameter: P_{rad} fraction
Tokamak: EAST

Non-disruptions

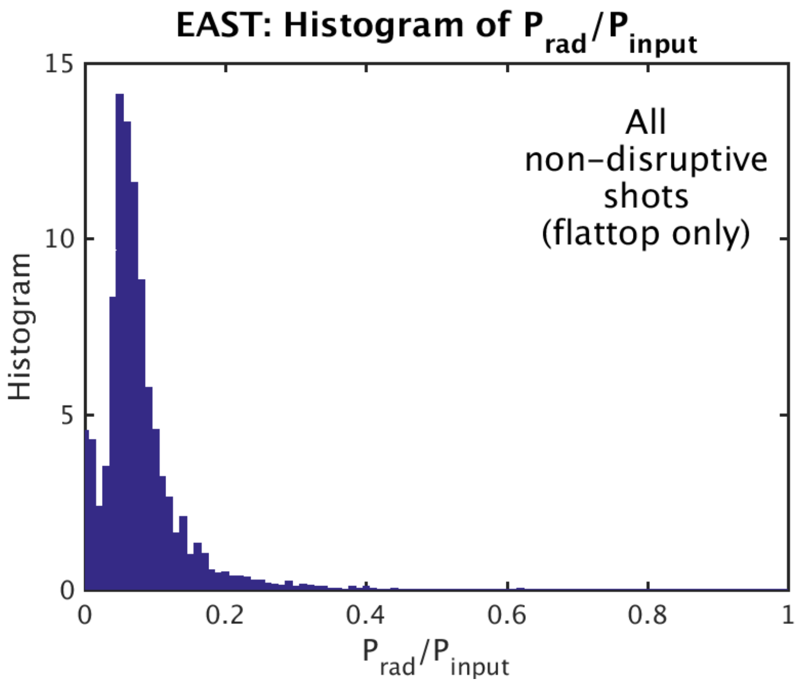

Disruptions

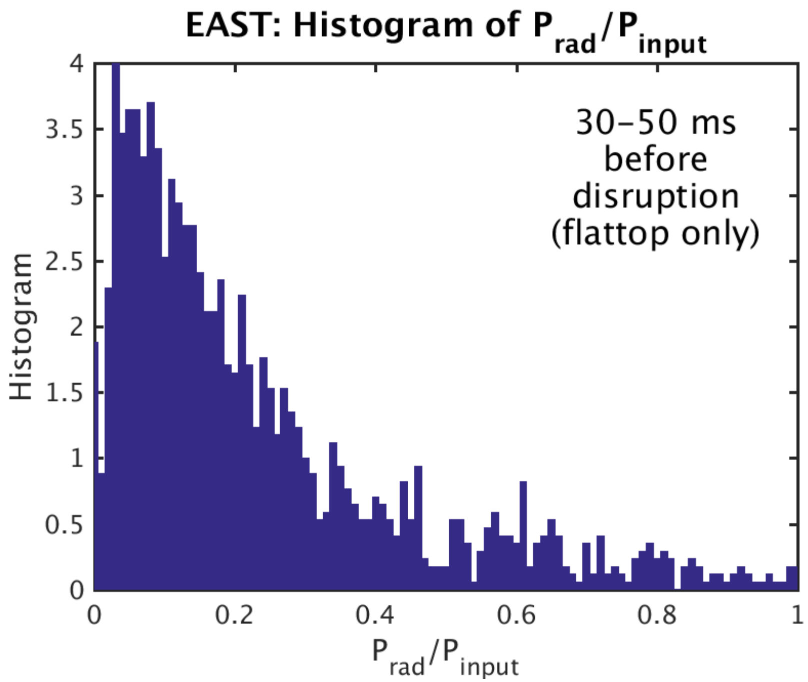

If we declare: P_{rad} fraction ≥ 0.35 is threshold for disrupt:

24.9% of disruptions are predicted with ≥ 30 ms warning time

1.0% false positive rate

Parameter: P_{rad} fraction
Tokamak: C-Mod

Non-disruptions

Disruptions

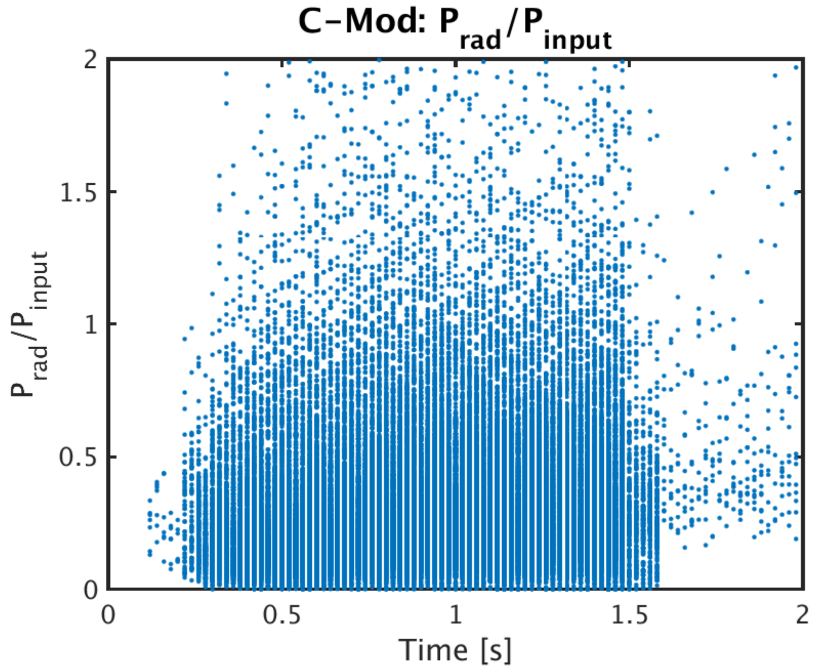

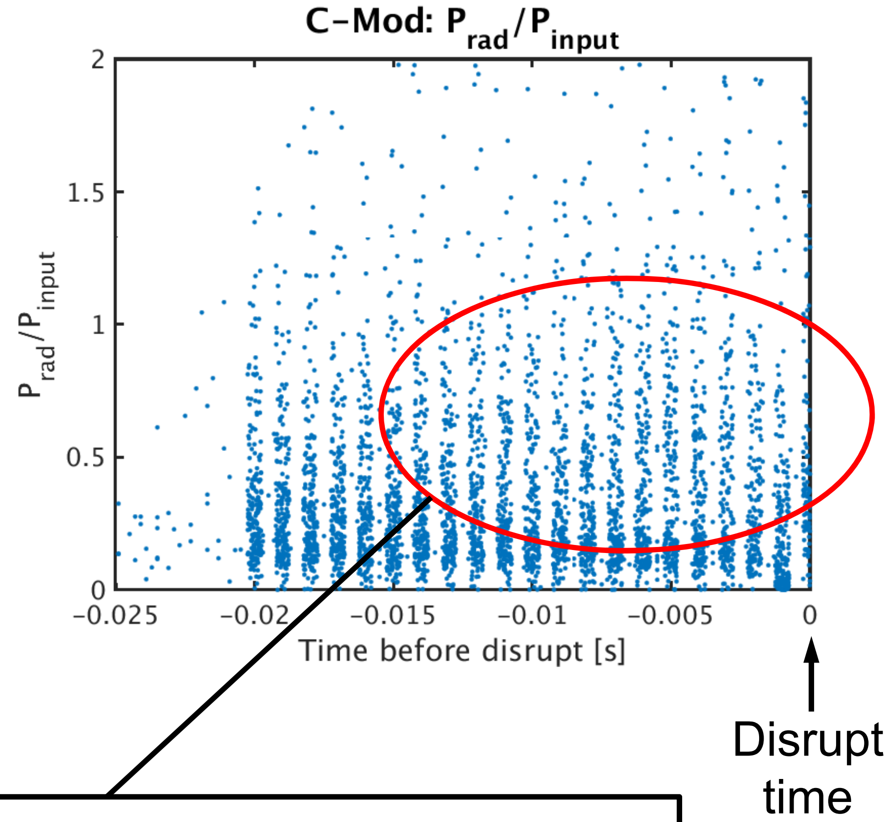

P_{rad} fraction values do ***not*** increase noticeably before disruptions occur

Parameter: P_{rad} fraction
Tokamak: C-Mod

Non-disruptions

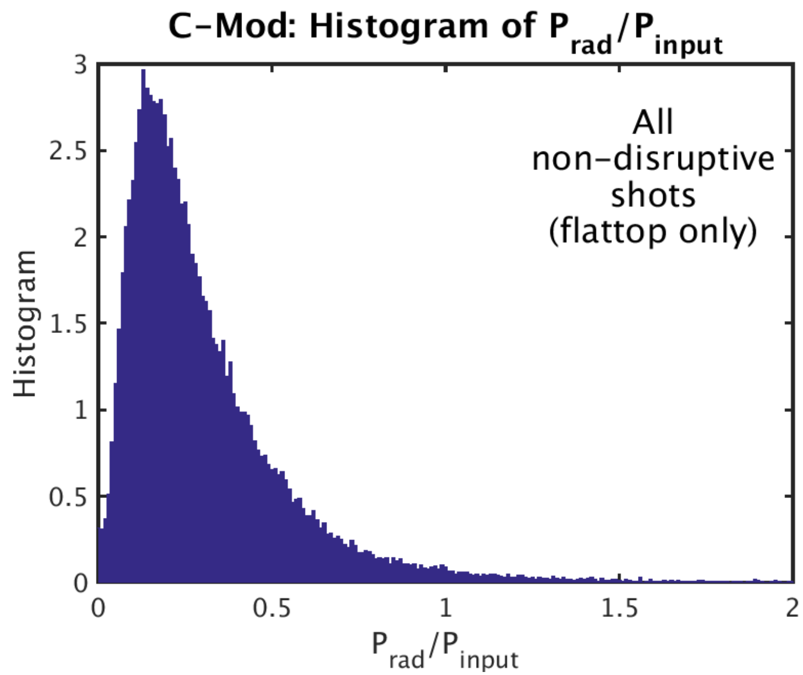

Disruptions

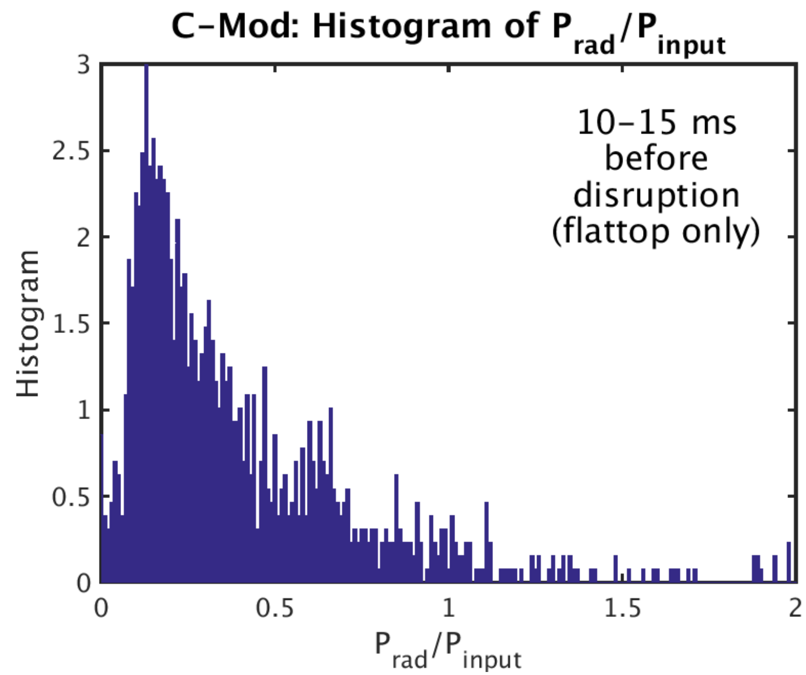

If we declare: P_{rad} fraction ≥ 1.4 is threshold for disrupt:

- 4.0% of disruptions are predicted with ≥ 10 ms warning time
- 1.4% false positive rate

Parameter: I_p error
Tokamak: EAST

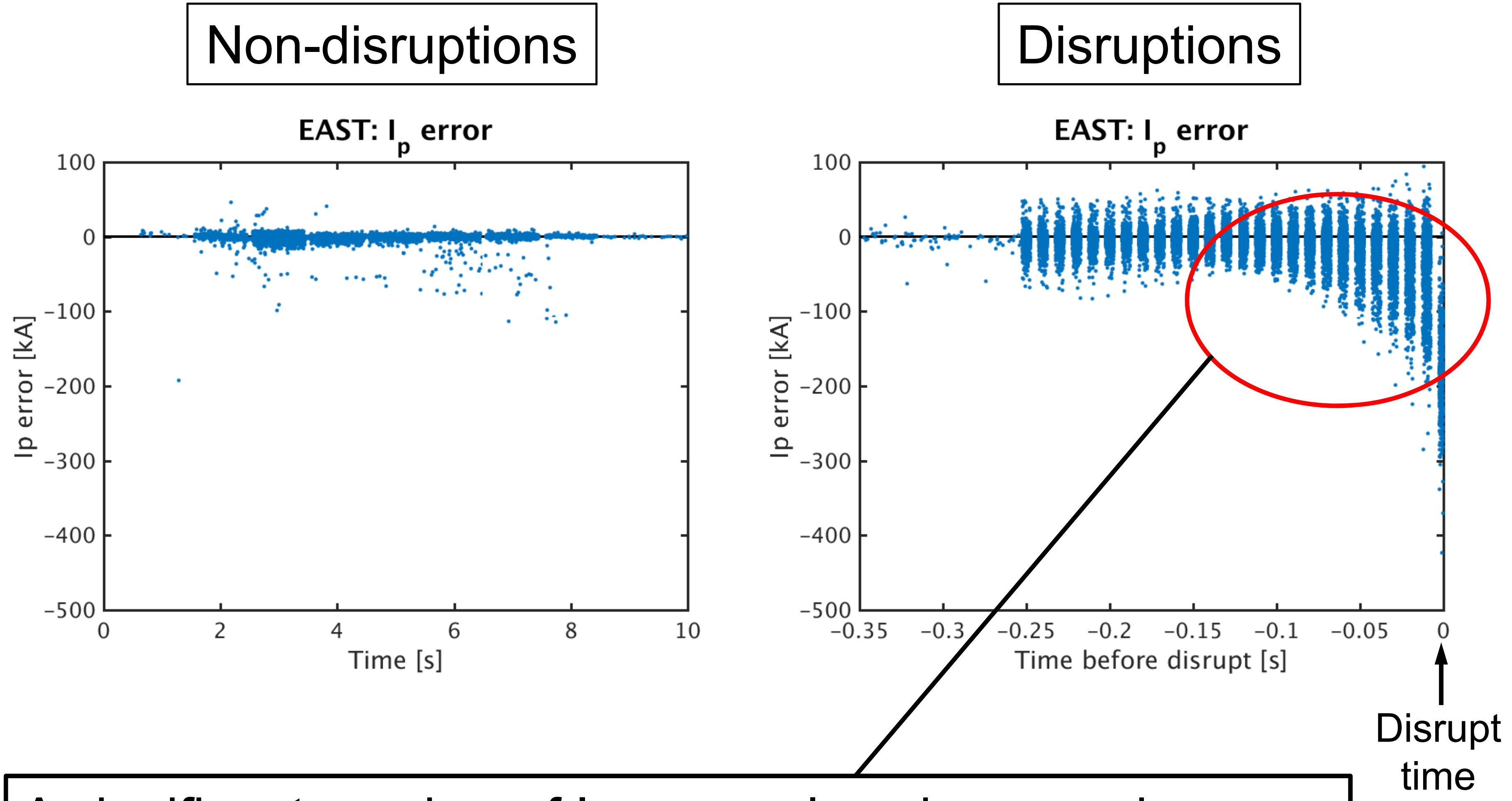

A significant number of I_p error values increase in magnitude during the ~100 ms before disruptions occur

Parameter: I_p error
Tokamak: EAST

Non-disruptions	Disruptions

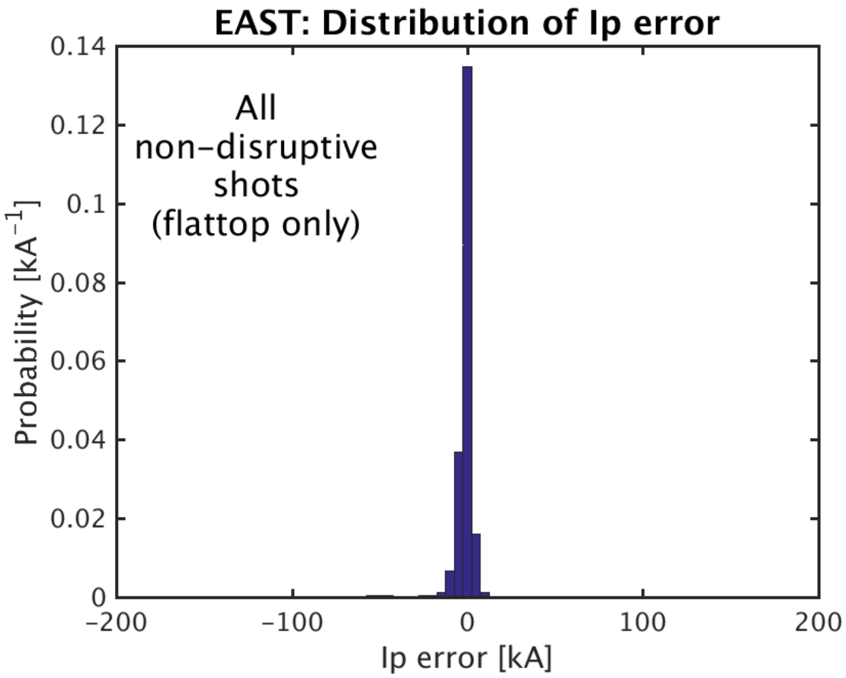

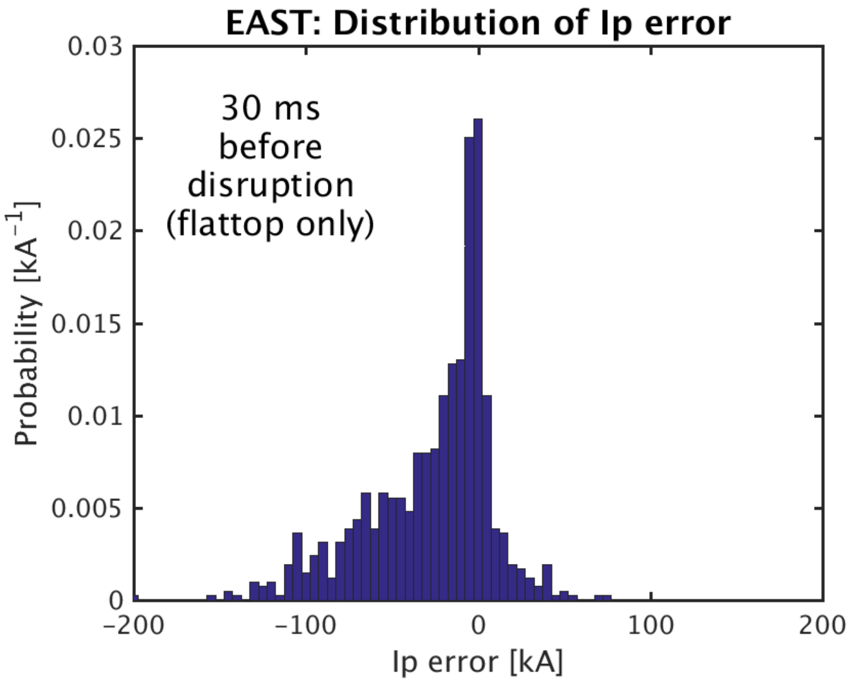

If we declare: Ip error ≤ -30 kA is threshold for disrupt:

34.2% of disruptions are predicted with ≥ 30 ms warning time

0.9% false positive rate

Parameter: I_p error
Tokamak: C-Mod

Non-disruptions	Disruptions

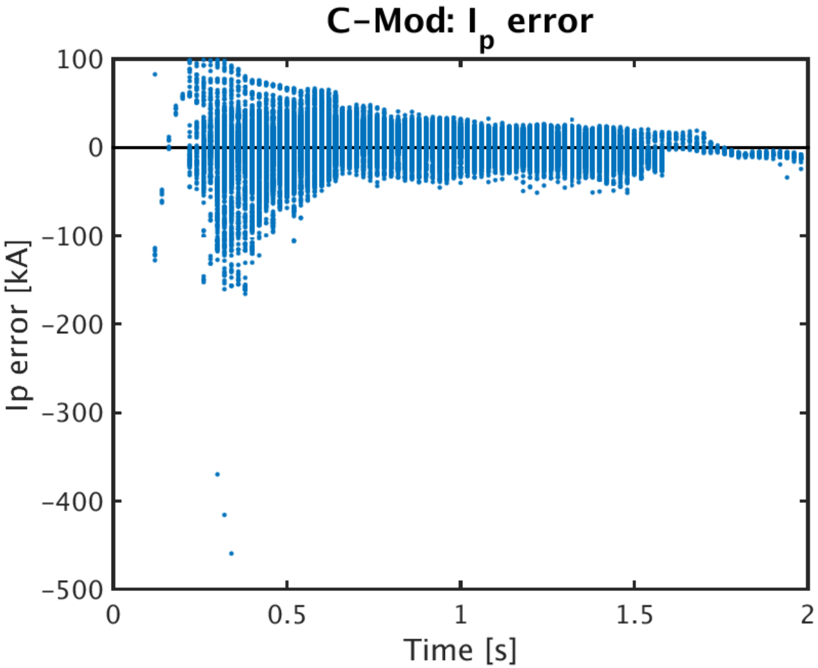

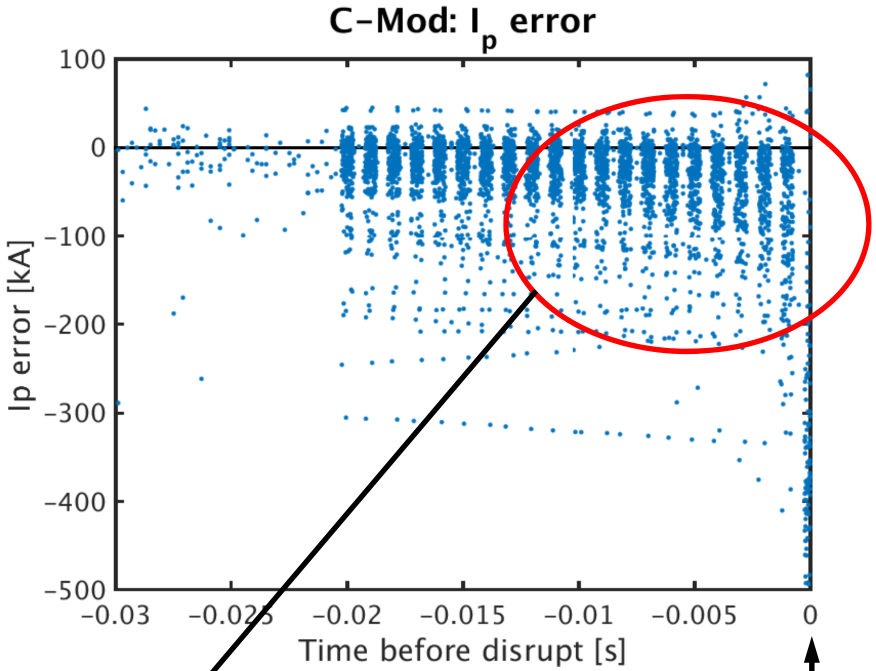

Disrupt time

I_p error values do not increase significantly until just ~10 ms before disruptions occur

Parameter: I_p error
Tokamak: C-Mod

Non-disruptions

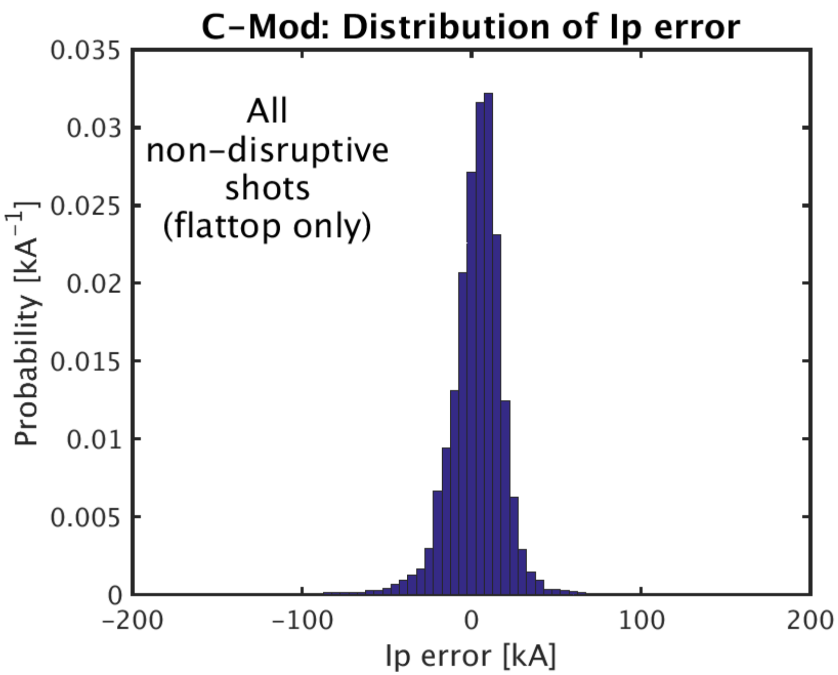

Disruptions

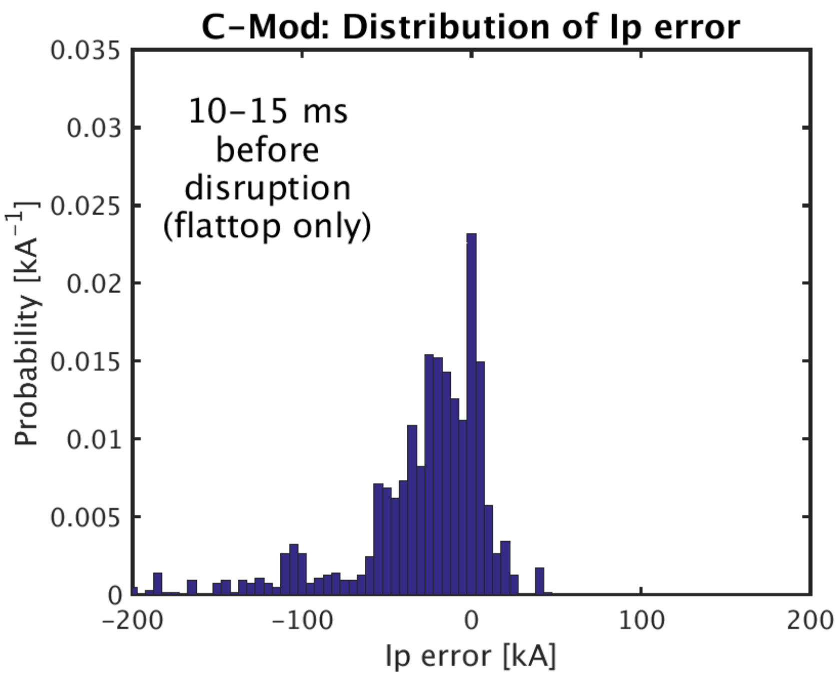

If we declare: Ip error ≤ -60 kA is threshold for disrupt:
- 15.7% of disruptions are predicted with ≥ 10 ms warning time
- 0.9% false positive rate

Summary and Conclusions

We have examined several disruption parameters using our C-Mod and EAST disruption warning databases. More relevant parameters are still being added (locked mode signals, etc.)

- So far, our studies show that these parameters provide a useful warning of impending disruptions on EAST, with $\geq$ 30 ms warning time
- But these parameters do a ***poor*** job of predicting disruptions on Alcator C-Mod with useful warning time

The faster timescales could be partly due to small size. But C-Mod "control room" experience is that most disruptions are caused by small moly injections, with no warning signs.

Could this be a general issue with high energy density, high-Z tokamaks, including ITER?

Application of machine learning techniques to our DIII-D disruption warning database

C. Rea, R. Granetz

MIT Plasma Science and Fusion Center

the two main subfields of Machine Learning are supervised and unsupervised learning

unsupervised learning

- uncover hidden regularities as **clusters** or **patterns**, or detect **anomalies** in the data

supervised learning

- an *a-priori* **label** is associated with each data sample

discrete label → **classification problem** → **binary** / **multi-class**

real-valued label → **regression problem**

➢ learning is not only a question of remembering but also of **generalization** to unseen cases

- **train dataset**
- **test dataset**
- **cross-validation dataset**

to determine disruption events with sufficient warning time it is possible to choose among a plethora of ML algorithms

- **statistical analysis of disruptions** has already been addressed in past years
  - P.C. de Vries et al. Nuclear Fusion 49 (2009) 055011
  - S.P. Gerhardt et al. Nuclear Fusion 53 (2013) 063021

- **Machine Learning "black box"** approach, through both supervised and unsupervised algorithms, was developed mainly at JET and also studied in real-time environment
  - **Artificial Neural Network** - B. Cannas et al. Nuclear Fusion 44 (2004) 68-76
  - **Support Vector Machine and Novelty Detection** - B. Cannas et al. Fusion Engineering and Design 82 (2007) 1124-1130
  - **Support Vector Machine** - G.A. Rattá et al. Nuclear Fusion 50 (2010) 025005
  - **APODIS, multi-tiered Support Vector Machine** - J. Vega et al. Fusion Engineering and Design 88 (2013)
  - **Manifolds and Generative Topographic Maps** - B. Cannas et al. Nuclear Fusion 57 (2013) 093023
  - **Generative Topographic Maps, APODIS and conformal predictors** - B. Cannas et al. Plasma Physics and Controlled Fusion 57 (2015) 125003

as first approach, we implement a Random Forests* algorithm to classify our dataset and gain further insights on its structure

- to obtain a **warning time related to the probability of disruption occurrence**, a methodology is first developed to solve the **binary classification** problem: **disrupted/non-disrupted**

- the **multi-class classification** problem is also studied, where the **time dependency** is included through the definition of class labels on the basis of the **elapsed time before the disruption** (i.e. "far from a disruption", "within 100 ms of disruption", etcetera)

- Random Forests are large collection of **decision trees**

*L. Breiman, "Random Forests", Machine Learning, 45(1), 5-32, 2001

graphical depiction of a single tree in a Random Forests

max_depth = 3

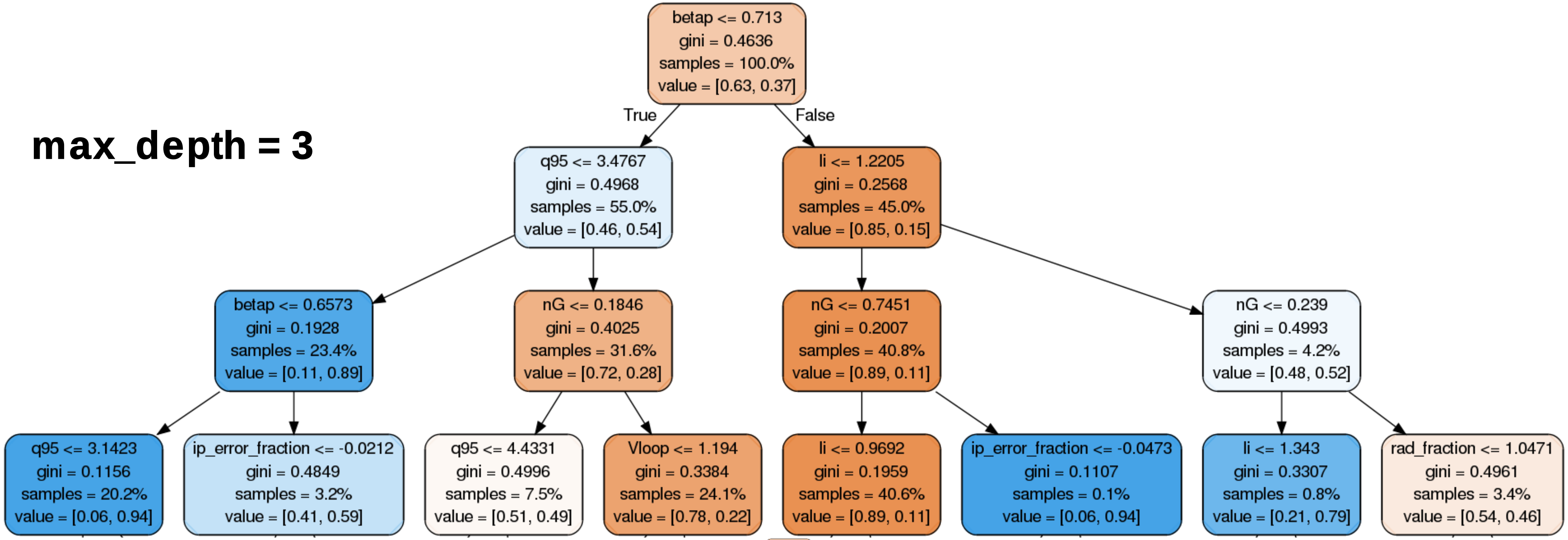

max_depth = 5

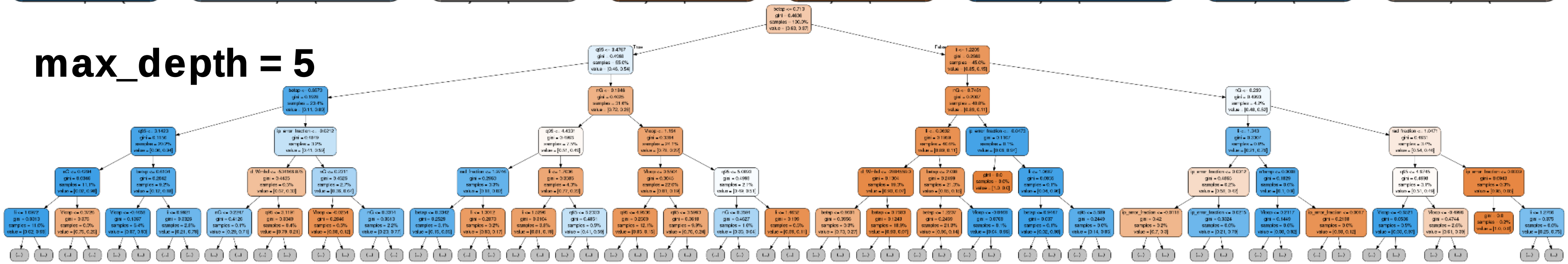

fully-grown tree

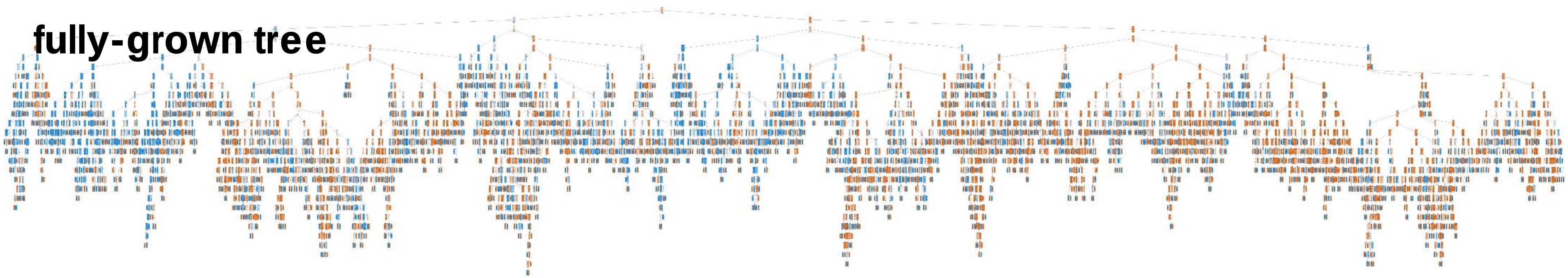

graphical depiction of leaf (i.e. final) nodes in a tree

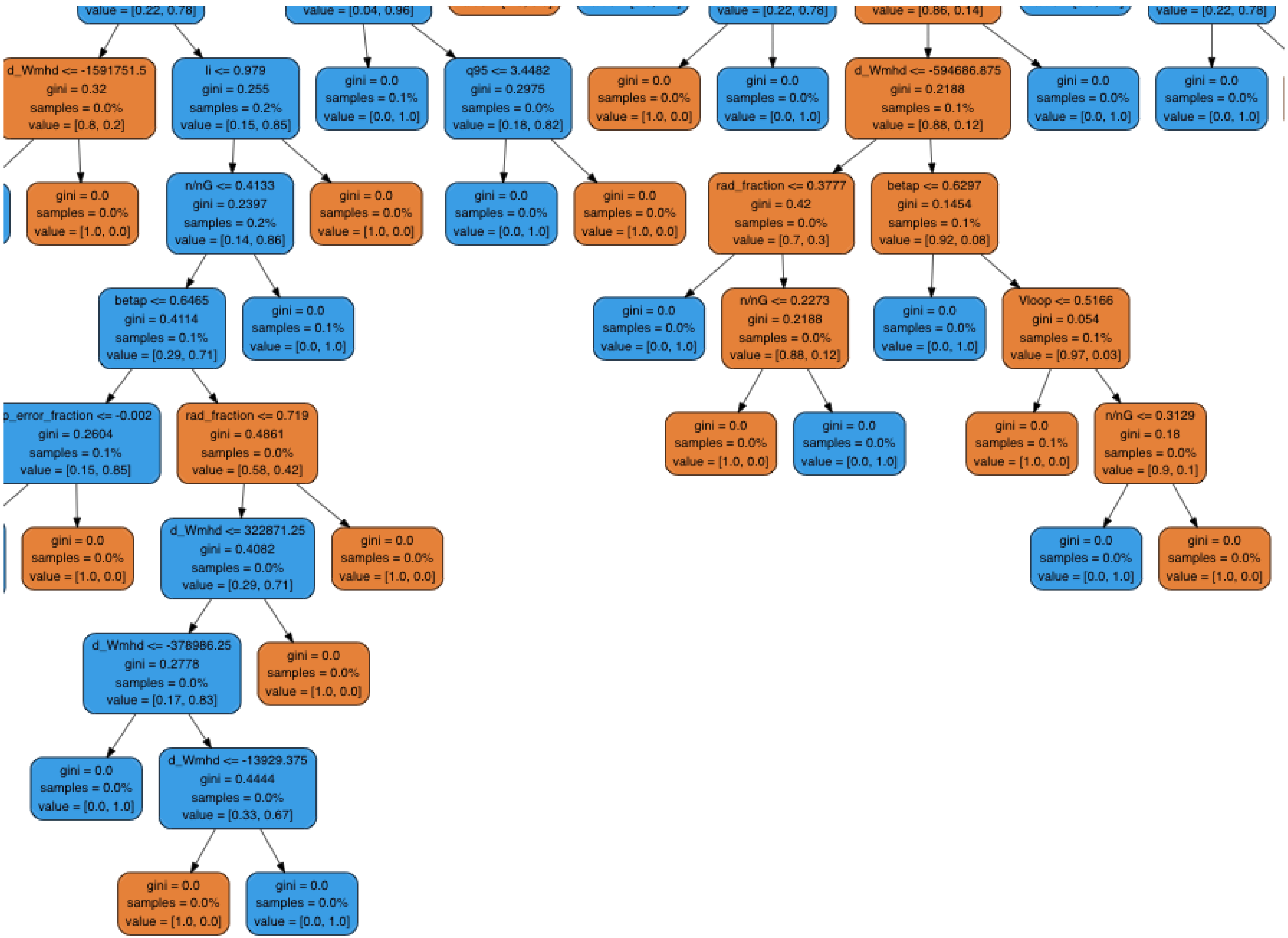

feature importance for Random Forests algorithm applied to the binary classification problem: disrupted/non-disrupted

- class labels: (0,1) have no time dependency
- mean accuracy of the model: ~ 0.95
- 500 estimators (trees)

```
Mean accuracy of the model: 0.949

Feature importances:
 1) q95                                   0.388240
 2) n/nG                                  0.153186
 3) betap                                 0.146960
 4) li                                    0.103943
 5) ip_error_fraction                     0.064097
 6) d_Wmhd                                0.046546
 7) Vloop                                 0.045887
 8) rad_fraction                          0.038884
 9) n1amp                                 0.012258
```

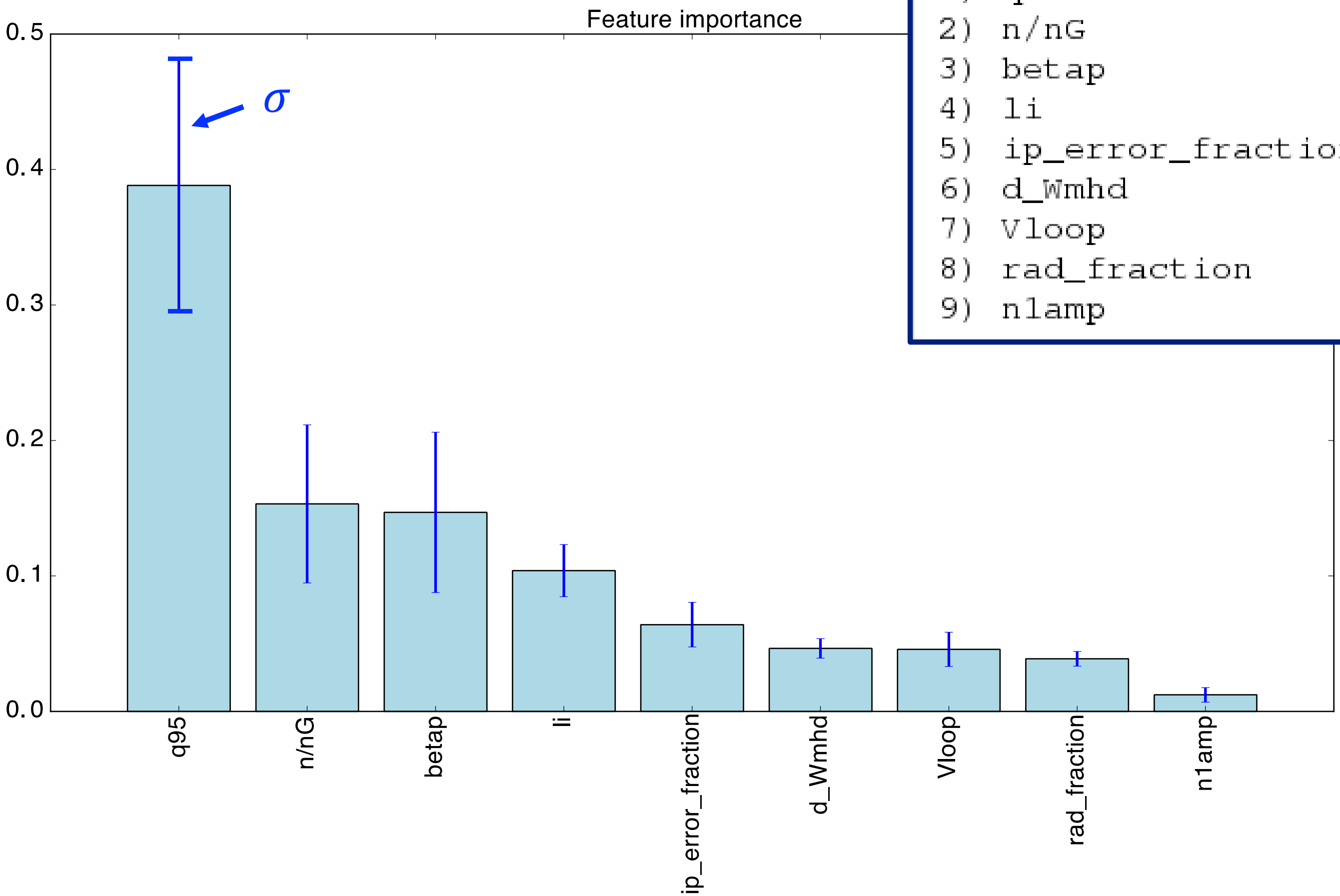

why q95 and n=1 amplitude have such different discriminative power and relative importance

- q95 probability distributions show major differences between the disrupted and non-disrupted discharge data
- while for the n=1 amplitude data, disregarding the peak at zero, it's true that the difference between disruptions and safe discharges does exist but it is very slim in terms of probability density.

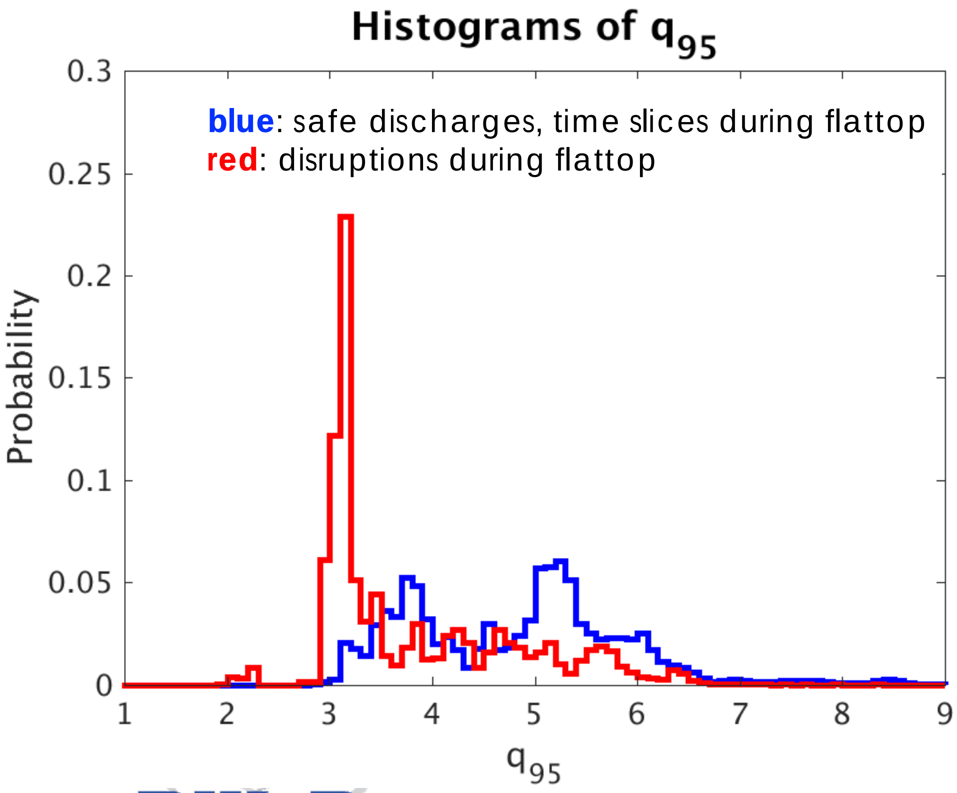

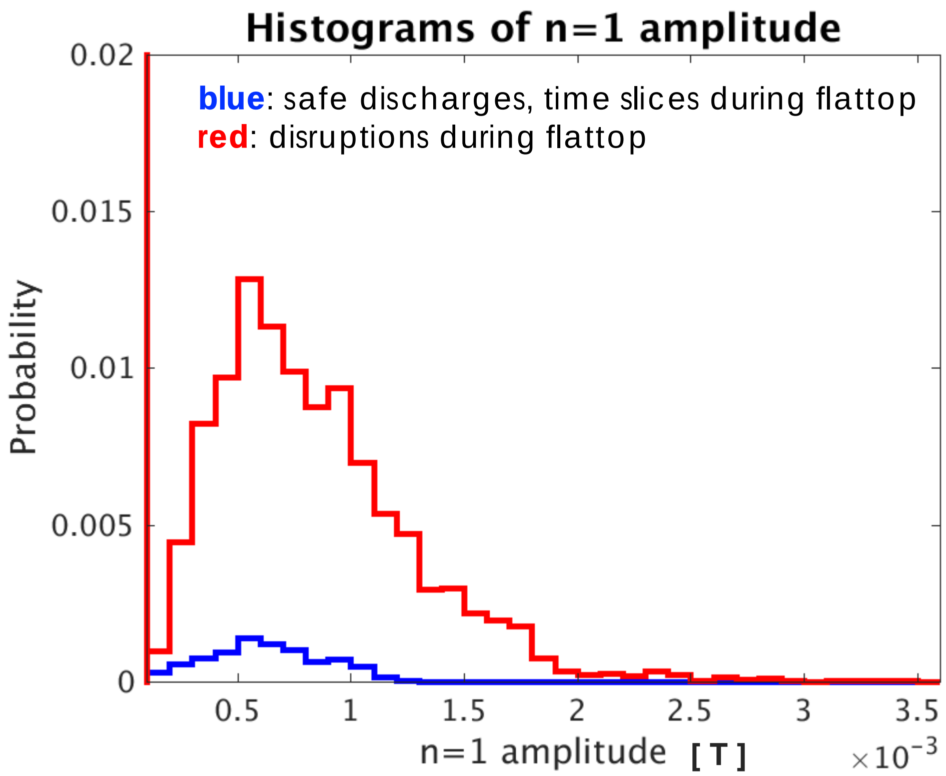

feature importance for Random Forests algorithm applied to the multi-class classification problem with the induced time dependency

- definitions of class labels (0,1,2) are given according to the elapsed time before the disruption
- dataset consists of all disrupted discharges (171 shots)
- mean accuracy worsens: ~ 0.85
- 500 estimators (trees)

```
Mean accuracy of the model: 0.848

Feature importances:
 1) q95                                   0.175944
 2) n/nG                                  0.175685
 3) li                                    0.145048
 4) betap                                 0.127457
 5) d_Wmhd                                0.114103
 6) ip_error_fraction                     0.105188
 7) Vloop                                 0.069271
 8) rad_fraction                          0.056007
 9) n1amp                                 0.031298
```

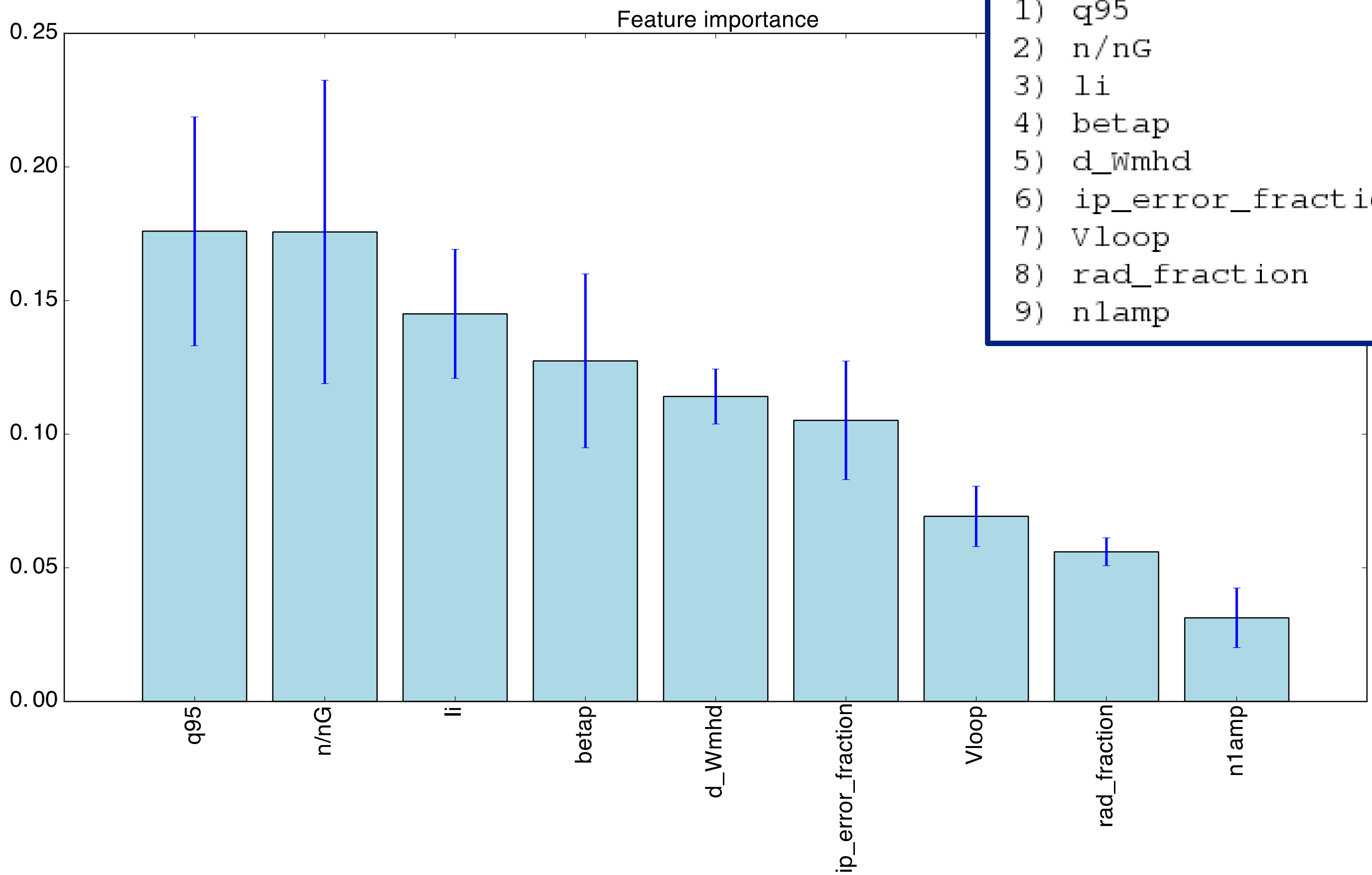

confusion matrix is used as an accuracy metrics to assess the model's capability to discriminate between class labels

binary classification

the dataset is composed of 59% **non-disruptive** time slices and 41% **disruptive** time slices

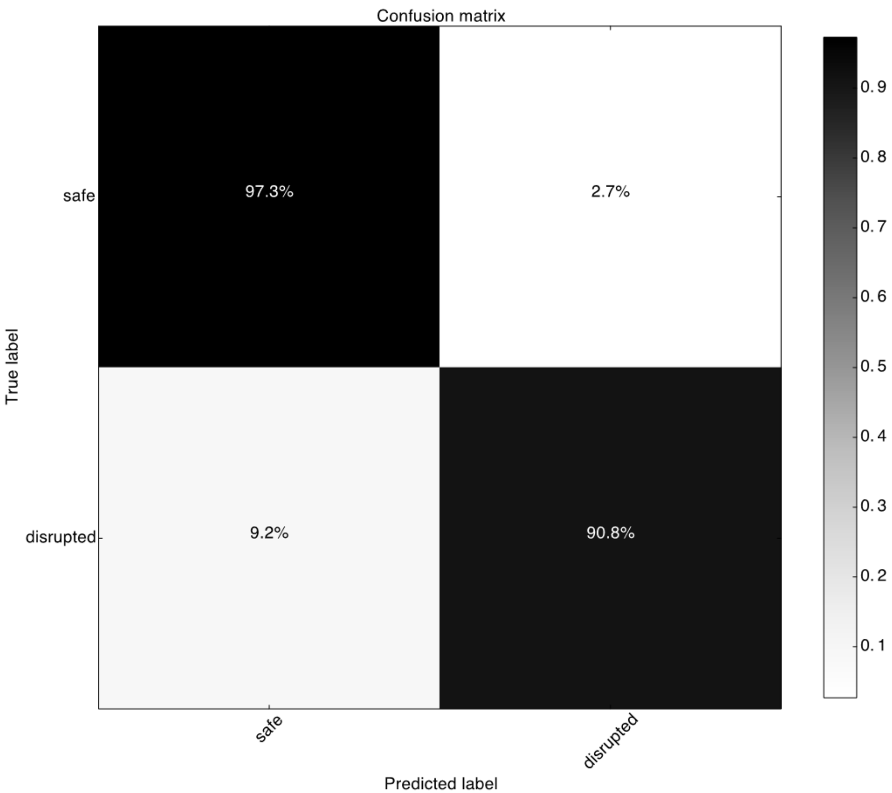

multi-class classification

the dataset is composed of **only disrupted** time slices

"far from disr" : time_until_disrupt > 1s
"in-between": 0.1s < time_until_disrupt < 1s
"close to disr" : time_until_disrupt < 0.1s

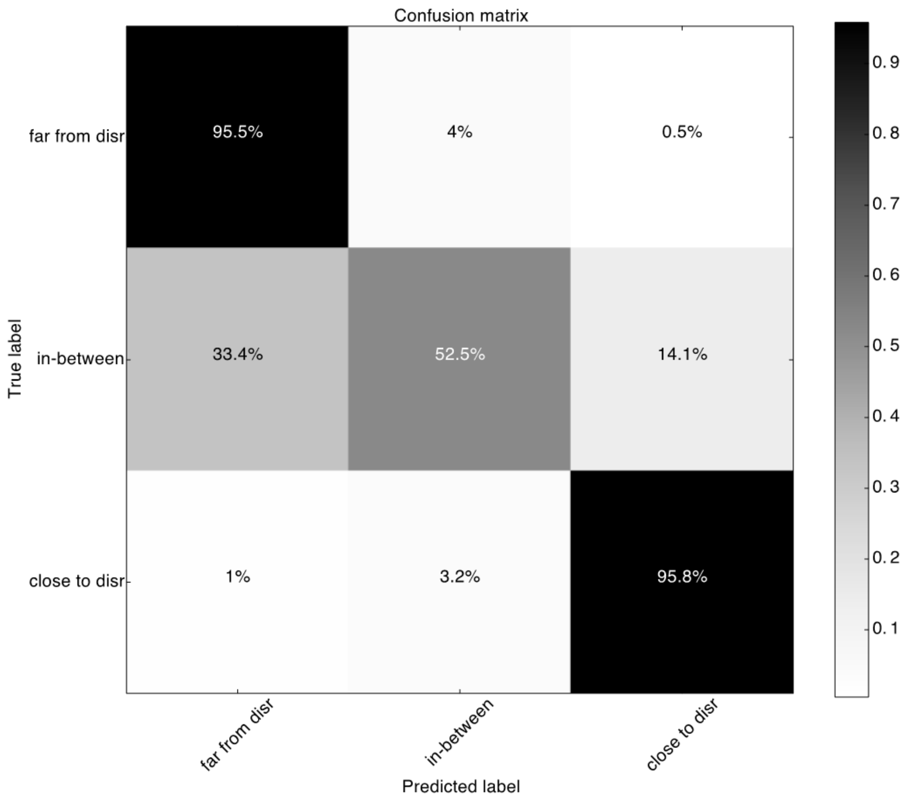

confusion matrices for multi-class classification: comparison between different datasets

multi-class classification

"far from disr" : time_until_disrupt > 1s
"in-between": 0.1s < time_until_disrupt < 1s
"close to disr" : time_until_disrupt < 0.1s

the dataset is composed of **disruptive** time slices; **non-disruptive** time slices populate the **far from disr** category

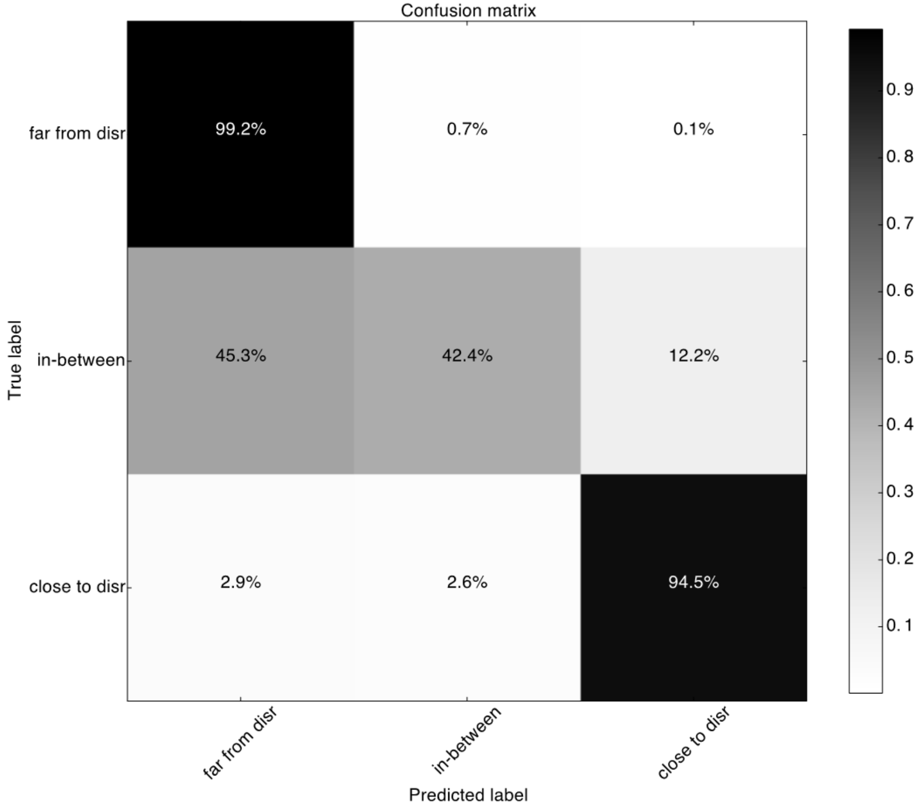

the dataset is composed of **only disrupted** time slices